Response to comments RC3

We have now reviewed the comments by RC3. We appreciate the suggestions and comments posed by the referee. Below we include the answers to all the questions and they were incorporated into the manuscript.

Please find below the response to each of their comments in *blue italics.*

Comment 1. The paper represents a continued interest in applying geophysical techniques to ecological questions. I think the authors do a great job at presenting the problem and application of GPR to this research question, however, they don't do a great job at highlighting potential limitations of the technique.

Authors: In the version reviewed by *We had already addressed the major limitations encountered in this study inserted in the conclusion section (pages: 12 and 13, lines: 31-33 and 1-3). Following the comment, we included some lines in the introduction section, highlighting potential limitations of the technique:*

"However, various factors affect detection of roots using GPR, such as root position, wood density and the conditions surrounding roots. These conditions include for instance, physical properties, altered or removed material, the volumetric water content, temperature, dissolved solids or salinity, the existence of regolitic material, and applied GPR wave frequency. These conditions may interfere with signal transmission and thus resulting in low-quality and difficult-to-interpret profiles (Table 1). For example, root zones in wet conductive soils, high-frequency waves are strongly attenuated limiting the resolution to detect roots and depth penetration (Butnor et al., 2012)" (page 3, lines 14-19).

Comment 2. I also feel the authors could have explained how they classified "noise" and how they dealt with that aspect in their methods.

Authors: *We implemented the "Bandpass filtering routine" to eliminate much of the noise in the radargrams. Noise seriously affects the judgement of reflective surfaces. However, noise can be removed by vertical high-pass and low-pass filtering. A high-pass filter, removes the low frequency signal content in the temporal dimension. It is used to remove* *low frequency data and horizontal banding due to system noise. Based on this comment, we extended the description of the filtering method of the signal-to-noise ratio following the steps described Butnor, J. R., et al. (2012) chapter. (pages: 7 and 8, lines 15-33 and 1-6). (pages: 7 and 8, lines 15-33 and 1-6).*

Comment 3. Finally, I worry they didn't provide enough details on the settings of the antenna (e.g., signal gain points), nor did they report any calibration of the antenna/method for their sites. All GPR practitioners will say that users must do some level of calibration to understand their site to adequately decipher their radiogram results. It's not clear if they have done this or just powered on the instrument and just used the factory default settings. I would recommend they provide some additional details before this is published.

Authors: *As suggested by the reviewer we have replaced the section "Data processing" by "Data processing and interpretation". The configuration to remove the DC component to offset the signal gain, and also were included the adjustment of other equipment parameters (pages: 7 and 8, lines 15-33 and 1-6). Regarding the calibration and validation of radargrams, we used in-situ roots for calibration (76 roots total). In Figure 2a we present the relationship between root diameter and signal emitted by the GPR system for all experimental plots. Also, in Table 3, we present values of roots measured in-situ as well the corresponding information from the GPR signal that we used for calibration and validation of roots (diameter and depth). The Table 3 represent a radargram of a pine-oak plot (Fig. S4).*

- ***Introduction***

Comment 4. The introduction was well written and presented a great overview of the topic. Unfortunately, the introduction lacked any mention of the real tradeoffs of using GPR in ecological issues.

Authors: *This comment was addressed on lines (Page 3, lines 14-19). The text describing these limitations is also shown in comment 1 above.*

Comment 5. I was disappointed the introduction lacked any clear description of the types of tree at the SSM or their typical root characteristics (e.g., tap root).

Authors: *Little is known about root morphology and distribution of these two particular species growing on shallow rocky soils. In page 4, lines 2-3, we added the following text addressing the reviewer's concern: "overall Quercus species exhibit dimorphic roots, while Pinus species display preferently superficial roots spreading horizontally (Kutschera & Lichtenegger, 2002)."*

Comment 6. Finally, the second objective "with the use of GPR, detecting roots of different diameter size classes growing at various depths in volcanic fractured rock" – Why just determine diameter? You could easily estimate root mass or architecture from this study and would likely be the most useful product for other studies/models to use (diameter is a poor indicator of age, mass, etc.).

Authors: *We thank the reviewer for this recommendation. However, we implemented geophysical tools in our studies, as a need to answer a research question about the operation of water redistribution (hydraulic lift) n this semi-arid rocky forest with shallow soil, question that arose from a previous study Rodriguez-Robles, U., Arredondo, J. T., Huber-Sannwald, E., and Vargas, R.: Geoecohydrological mechanisms couple soil and leaf water dynamics and facilitate species coexistence in shallow soils of a tropical semiarid mixed forest, The New phytologist, 207, 59-69, 10.1111/nph.13344, 2015.*

As such, we prepared the present manuscript only with the root diameter information we recorded to address the mentioned question.

- ***Methods***

Comment 7. Why were the plots circular? Circular data collection leads to some problems with interpreting such issues. There have been some companies (e.g., Tree Radar), that had to develop new methods to analyze tree trunk decay from GPR images collected around the trunk (in other words, in a linear transect, you can compare reflector intercepts, but in a circular scan pattern, you will have to deal with adjacent intercepts that will be dealing with different intercept angles at the edges). How did you account for this in your analysis?

However, with a circular pattern, you could determine if there is any overshadowing of rocks or other roots.

Authors: *For the present study, we used three different transect types to carry out the GPR tests for root survey. First, we implemented a radial transect oriented in four directions (NS, NE-SW, EW and SE-NW) within each experimental plot of 25 m diameter, using a 500 MHz antenna for the 12 experimental plots. Another transect consisted of the concentric sampling mentioned by the referee, each sampling included five concentric transects (0.1, 0.3, 0.5, 1.0 and 1.5 m between neighboring transects) around a Pinus cembroides tree anchored within an exfoliated rock using the 800 MHz antenna. The objective of surveys following concentric transects was to figure it out whether Pine located roots underneath the exfoliated rock as a source of humidity and nutrients as well as to observe how roots distributed roots away from the rock. In this case, we only worked with reflected hyperbolas that result from perpendicular roots to the GPR direction. Therefore we only used well defined reflected hyperbolas. Finally, the third transect type was established inside 8.5 x 6 m plots, consisting in seven parallel transects (spaced 1 meter) to observe horizontal axis elongation of roots in a mixed stand.*

This experimental arrangement was addressed in the section "2.2 Experimental plots" page 5, lines 4-79.

Comment 8. Just using 0.1, 0.3, 0.5, 1.0 and 1.5 m transects – its unlikely you could detect small diameter (~0.6cm) roots with a 500 MHz antenna or a 900 MHz antenna with such large gaps (especially with the higher frequency antenna).

Authors: *In transects of 1.0 and 1.5 m, we detected small diameter roots (0.6 cm) using the 800 MHz antenna. We validated with direct measurements of roots in situ the hyperbolic signal, to calibrate the radargrams.*

Comment 9. Did the soil sensors have any metal in them? If so, how did you deal with issues with signal attenuation?

Authors: *We understand the concern of the reviewer. The soil psychrometer sensors (PST-55), they are designed with high thermal conductivity materials. we installed the psychrometers with the axis of the sensor parallel to the soil surface and depending on the* *depth of soil pockets we installed the psychrometers of 12 - 15 cm deep. Before the surveys with GPR and ERT, we performed the measurement of the water potential and after that, the sensors were extracted for the geophysical surveys.*

Comment 10. On Page 5, when you talk about the principles of GPR, you could mention the resolution-depth-frequency tradeoff, but it might be better in the introduction.

Authors: *We took into account the reviewer's comments; the section was modified as follows: "The ground electrical conductivity, the transmitted center frequency, and the radiated power, all may limit the effective depth range of GPR prospection. Increases in electrical conductivity in the ground may attenuate the introduced electromagnetic wave, and thus its penetration depth decreases. However, higher GPR frequencies may provide improved resolution. Hence, operating frequency is always a trade-off between resolution and ground penetration (Aditama et al., 2017)." Page 3, lines 1-5.*

Comment 11. What about air gaps? Wouldn't volcanic rock have a large number of "air bubble" gaps? How would you deal with issues associated with air gaps? From my experience, this causes change in the signal speed and can cause issues with your gain settings and therefore interpretation.

Authors: *As mentioned in the methods, the study was carried out in the SSMVC that represents the remnants of one of the most voluminous rhyolitic volcanic events on Earth (McDowell and Keizer, 1977), formed by massive lava spills of rhyolitic composition (Portezuelo Latite and San Miguelito Rhyolite). Rhyolite is an extrusive igneous rock, making it impermeable and void of porosity. The weathering of this rock is by lapping, so there are no abrupt changes in the rock surface. Still, to minimize issues associated with air gaps, we set the "set zero level" to compensate for signal gain. In addition, the "auto stacking" was configured for highest data quality and optimized speed performance.*

To run the root surveys, we first configured the antennas [time windows (400 ns), stacks (auto), sampling frequency (1120 MHz), point distance (0.001 m) and velocity (110 m/µs)] and used a pulling system and a measuring wheel fitted to the mounting block on the back of the shielded antenna. The antenna was dragged along the transect trying to always maintain it in close contact with the soil.

Comment 12. In page 6, section 2.5, to what depth?

Authors: *We added the depths as shown in the following text;* ***"****From October to December 2012, we examined the frequency, size, position and depth range of roots with 2.5 to 7.5 cm diameter in the top soil and under exfoliated rocks, using the GPR 500 MHz antenna and working with a 2.5 m depth window. To characterize the exfoliation of weathered bedrock soil, and to differentiate between the exfoliated rock base and potential root axes (0.6 to 4 cm diameter) underneath rocks, we used the GPR 800 MHz antenna, exploring at 1 m depth". (Page 6, lines 25-28).*

Comment 13. How did you deal with the immediate ground reflection from the antenna? Were there any gaps (due to micro topography? If so how did you deal with this?

Authors: *To deal with this problem, we focused on signal processing from a reduced clutter that better represent the geometry of roots (as mentioned in response to Comment 2, addressed in section 2.6). It is worth noting that we carried out the root surveys using MALA shielded antennas (consists of both transmitter and receiver antenna elements in a single housing) obtaining signals and reflection data that are cleaner for interpretation.*

Comment 14. Page 6, line 26-31, over the 8month sampling period, did you collect the ERT at the same time as the GPR? Since soil water content can change so rapidly in arid/semi arid regions, this would be important especially since changing moisture levels will impact your dielectric constant.

Authors: *Thanks for the observation, the GPR surveys were carried out in October 2012 during a drought period (45 days of soil drying, previous to the survey) to assure cleaner signals and reflectance of roots in these complex soils. ERT profiles in contrast, were carried out one year later, beginning in a wet period (October 2013) and lasting for eight months until the dry period (May 2014), with the objective as defined for this experiment to "determine if resistivity tomography help to detect the spatial and temporal variability of soil moisture beneath vegetation patches" and to "describe the role of weathered bedrock in forest ecosystems colonizing shallow rocky soils.*

With this arrangement we were able to overlap GPR and ERT profiles and show the relationship between root location, low soil resistivity (greater water availability) and greater bedrock fracturing, as shown in the figures 5 and S5.

Comment 15. The manuscript makes no mention of site calibration for your equipment/method. From my experience, you need to calibrate GPR to the site conditions, especially with respect to signal gain points. It was unclear how many gain points were used and if they changes between plots (using the "automatic gain detection feature often isn't the best for mid to high resolution studies where you want to compare between plots).

***Authors:** In section 2.6 it is mentioned both the calibration method as well as the radargam processing using RadExplorer software (page 7: lines 15-33 and page 8: lines 1-6). To calibrate and validate the root survey method we proceeded as follows; "Root identification in the radargrams was a stepwise process; first, roots were recognized at the locations where hyperbolas of reflected waves had higher amplitudes compared to those in the surrounding area (Cui et al., 2011). Then, to determine the diameter and depth of those roots, the time interval between zero crossings (ns, time interval for maximum reflected wave) was extracted at the points of hyperbolas, where roots had been identified previously. The detection frequency for the number of roots identified in the radar profile was calculated along each transect for five root diameter classes (< 3.0, 3.0 – 4.0, 4.0 – 5.0, 5.0 – 6.0, and > 6.0 cm). Finally, for calibration purposes, individual roots (total of 76) were excavated to determine their depth and diameter in-situ (Table 3, Fig. 2a). (Section 2.5, pages: 6 and 7, lines: 29-31 and 1-4).*

Comment 16. Page 7, line 6 – how did you determine unwanted signal (noise)? Any criteria? This would be useful for readers to understand this step in case they wanted to use this methodology. I would suggest looking at or referencing methods listed in the book "Measuring Roots: An Updated Approach (Springer; Editor: S. Mancuso - ISBN 978-3-642-22067-8) or "Handbook of Agricultural Geophysics" (CRC Press; Editors: B> Allred, J. Daniels, M.R. Eshani - ISBN 9780849337284).

***Authors**: Answer to this question was already addressed in comment 2. However, based on this comment, we have reorganized the section as indicated by the reviewer and also included the references for the signal-to-noise ratio issue described in the chapter of*

Butnor, J. R., et al. (2012). Using Ground-Penetrating Radar to Detect Tree Roots and Estimate Biomass. Measuring Roots: An Updated Approach. S. Mancuso. Berlin, Heidelberg, Springer Berlin Heidelberg: 213-245. (pages 7 and 8, lines 15-33 and lines 1-6).

Comment 17. Did you do any ground truthing of this method? This would be important to know what depths you are really reaching with this method. Some past studies have inserted a metal reflector pate at a known depth (e.g., 50cm) to ensure proper calibration of the data. Otherwise you are just making assumptions of how deep you are penetrating. I realize you did dig up some surface roots for a comparison, but differences in the soil, air gaps, variations in soil moisture, etc. can speed up or retard the signal travel time resulting in changes in depth interpretations.

Authors: *For calibration purposes, individual roots (total of 76) were excavated to determine their depth and diameter in-situ (Table 3, Fig. 2a). Using the "Tools / Depth Calibration" tool of the ProEx system, in-situ, we calibrated the depth of GPR radargam with that obtained by the excavation.*

Comment 18. Why not use a higher frequency antenna like 1500 or 2000 MHz since most of your roots are in the upper 50 cm of the soil?

Authors: *Limited by ground conditions (e.g., leaf litter, weathered bedrock regolith), we decided to work with the 500 and 800 MHz antenna. Following a rigorous processing in the Rad Explorer, we had obtained good results with the 800 MHz antenna for these floors with high presence of needles. Also, the use of 1500 or 2000 MHz antennas introduces a lot of noise coming from superficial debris and roots from the understory vegetation.*

Comment 19. Soils and root systems are highly variable and roots tend to crises cross/overlap areas in the soil, how did you partition roots out in the radar where they overlap (or grow side by side) and not consider them as 1 root, rather than 2 smaller roots). With such a low freq. antenna your diameters could be smaller roots in a group, rather than one 2.5 cm diameter root.

Authors: *To solve the problem due to the hyperbolas overlapping as well to identify the correct position of roots, we applied a Stolt F-K Migration routine. With the application of* *the Stolt F-K Migration routine we were able to restore the real location and shape of reflecting boundaries in a section plane. On the other hand, to determine the wave propagation velocity, we relied on the "Hyperbola" tool (Rad Explorer software) in order to determine migration velocity.*

Thus, after the Stolt F-K Migration routine was applied, if resulted reflections were not clear to interpret, that section was omitted.

- ***Results***

Comment 20. Page 8, line 26 – The authors suggest you could track elongation over time, but I doubt you could detect this with the sampling frequency and the reported diameter sizes, unless these are fast growing trees.

Authors: *The reviewer is correct, what we describe in this lines is the horizontal distribution of a root rather than its elongation. With the 500 MHz antenna, we detected the horizontal distribution of a root axis of Pinus cembroides in a 8.5 x 6 m plot running parallel transects (Figure 3 B). Through in situ excavations we were able to validate the hyperbolas reflected in the radargrams.*

Comment 21. Its' unclear how the authors dealt with the shadowing from rock fragments and potential gaps or microsites of moisture in a crevice in their radiograms?

Authors: *The GPR surveys were carried out during a period of drought (October 2012), to minimize signal noise in the radargrams and facilitate their interception. However, a limitation of using the GPR technology, relates to the interpretation of GPR images. To reduce this problem and when the conditions at the site allowed, following a GPR survey we proceeded validation through excavations removing soil and removable rocks as shown in the following figure.*

In the image is observed (after soil and rock remotion), a pair of roots of Pinus cembroides tree (anchored to a volcanic rock) that served to calibrate radargrams for the radial transects.

Comment 22. Page 9, line 11, its unclear what the authors mean by "spotted primarily" tree roots – what else was detected? this leaves some doubt in the detection analysis.

Authors: *Regarding the observation of reviewer, we refereed to the noisy signal generated by leaf litter accumulation under and on top of exfoliated rocks.*

Comment 23. How did the authors tease out species specific information? (e.g., Page 9, lines 13-19)? Were these monoculture patches of species?

Authors: *The reviewer is correct, the experimental study was set up in a pine-oak forest. Along a 2.5 km long transect we established a total of 12 circular experimental plots of 25 m diameter with four replicates for three types of forest stand types (pine, oak, and mixed stands). Page 5, lines 4-9.*

Comment 24. Page 9, line 5, wouldn't you need less than a meter for the 500 MHz to detect 0.6 cm roots? the 900 would likely detect this size range.

Authors: *Roots smaller than 1cm in diameter were only detected with the 800 MHz antenna in our case.*

Comment 25. Page 9, line 24-25 – could this finding be due to the differences in rooting strategies in Oaks and Pine species?

Authors: *The reviewer is correct, we assume that Pinus cembroides have a more limited geospatial niche than Quercus potosina and this is due to differences in rooting strategies between Oaks and Pine.*

Comment 26. Page 10, line 1 – how long did the water infiltration signal last? Also, when was this objective/phenomena studied? This could matter because the transpiration and plant water demands could change the interpretation of the duration of the perturbation.

Authors: *This was an additional test only to demonstrate the potential of the geophysical methods to detect short-term horizontal and vertical distribution of water in the substrate (e.g., in response to a rain pulse). We have re-worked the objective 4 (page 4, lines 17-18). Radargrams showed both a clear infiltration horizon at approximately 50 cm depth and a remarkably rapid horizontal displacement of this injected water. The signal appeared only 150 minutes following water injection and it was not homogeneous among all vegetation patches.*

- ***Discussion***

Comment 27. Page 10, line 22-23, I agree with the dual frequency approach given differences in sites and a method I would use (the art of the method), but again, you need to do custom your method to your site (ground truthing/validation).

Authors: *Regarding this reviewer comment, we can comment that we made calibration curves on each stand type, using root diameter (cm) and time interval (ns), as shown in table 4 and figure 2a. We were very careful in the calibration and validation of the method for each stand, following our configuration method.*

- ***Tables and figures***

Comment 28. Table 1 – I doubt they are seeing 0.6 cm diameter roots with the lower frequency antennas in this rocky soil substrate. Past studies have achieve this only with 1500-2000 MHz antenna only in ideal soil settings (sandy soils).

Authors: *We observed hyperbolic reflectances for roots smaller than 1cm using the 800 MHZ antenna, in the concentric transect arrangement (figure 4b) transect at 150 cm (letter "b").*

Following the filtering process presented in section 2.6 (pages 7 and 8, lines 17-33 and 1-6), we were able to eliminate and greatly improve the noise in the radargrams to facilitate interpretation. An example is shown underneath: a) Raw radargram; b) DC removal and correction of time zero c) Background removal and Bandpass filtering.

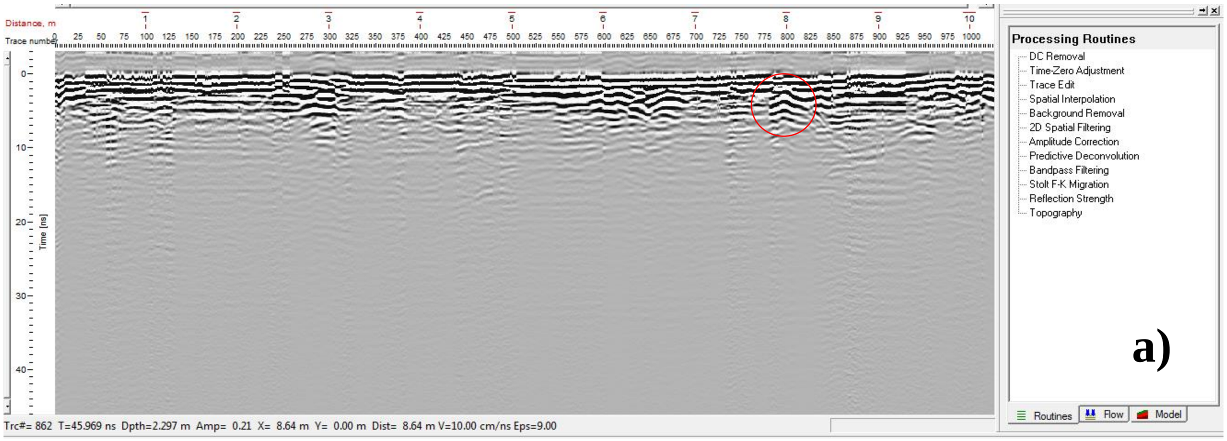

```
Trc#= 862  T=45.969 ns  Dpth=2.297 m  Amp=  0.21  X=  8.64 m  Y=  0.00 m  Dist=  8.64 m V=10.00 cm/ns Eps=9.00
```

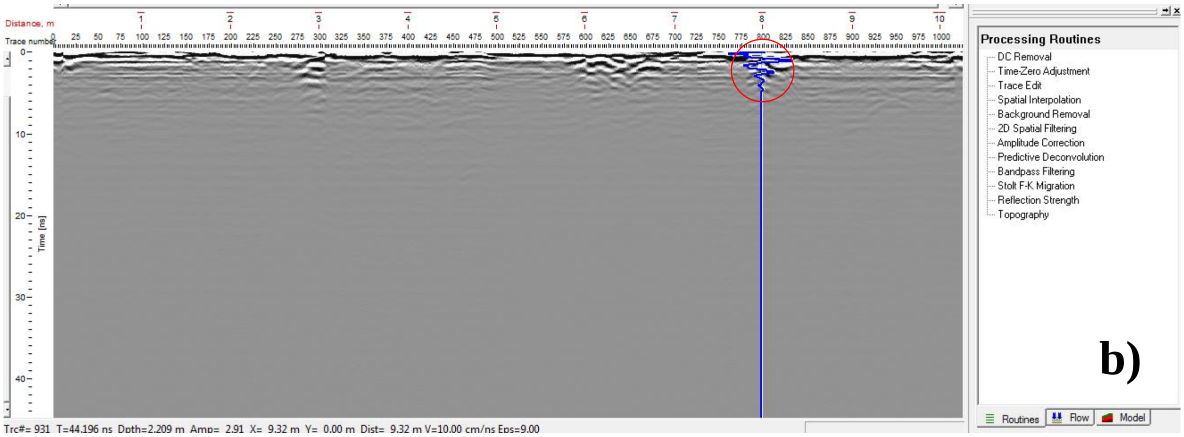

```
Trc#= 931  T=44.196 ns  Dpth=2.209 m  Amp=  2.91  X=  9.32 m  Y=  0.00 m  Dist=  9.32 m V=10.00 cm/ns Eps=9.00
```

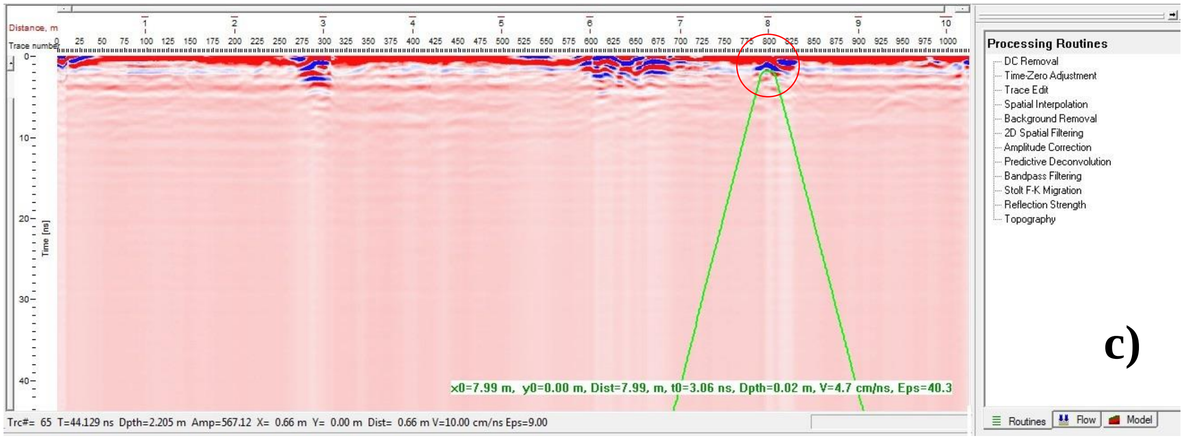

x0=7.99 m, y0=0.00 m, Dist=7.99, m, t0=3.06 ns, Dpth=0.02 m, V=4.7 cm/ns, Eps=40.3

Trc#= 65 T=44.129 ns Dpth=2.205 m Amp=567.12 X= 0.66 m Y= 0.00 m Dist= 0.66 m V=10.00 cm/ns Eps=9.00

Comment 29. Table 4 – the authors say "used for calibration" but don't really explain what they mean here? Also, It would be useful to show those regressions here.

Authors: *We thank the reviewer for this observation. Overall calibration method was explain in comment 15. Additionaly, direct measurements of root diameters were obtained from 4 different profiles. From each profile, we also conducted excavations of at least 4 roots in situ. For calibration for root diameter studies when applying the 500 MHz antenna we used the 12 experimental plots, whereas when surveying with the 800 MHz antenna we used the five concentric profiles for lateral root distribution underneath exfoliated rocks. For each of the profiles (500 and 800 MHz), roots were excavated and directly measured. In Figures 3, 4 and S4, roots used for GPR calibration are indicated with letters. Regressions were carried out with in-situ roots at different depths with those detected in the profile.*

Table 4 including parameters of linear regression was extended.

Type of sampling	**GPR systems**	**Stand**	**Intercept ± 1SE**	**Slope ± 1SE**	**R^2**	***P***
Radial	500 MHz	Pine	0.3610 ± 0.3751	5.7890 ±0.4473	0.92	<0.0001
Radial	500 MHz	Oak	-0.0013 ± 0.4234	5.7736 ± 0.4309	0.92	<0.0001
Radial	500 MHz	Mixed	-0.0536 ± 0.1506	6.0195 ± 0.1712	0.98	<0.0001
Concentric	800 MHz	Pine	-2.0910 ±0.1273	6.2450 ±0.1839	0.98	<0.0001

Comment 30. Figure 1 – the rockiness of the soil, and possible air gaps, would make signal processing very difficult here, each plot would need to be calibrated.

Authors: *Answer to this question is similar to that posed for comment 28.*

Comment 31. Figure 2 – what's the age class of the trees?

Authors: *In table 2 we have included a column with the estimated age of trees based on ring growth.*

Stand	***n***	**DBH (cm)**	**Age (years)**	**Tree height (m)**
Pine/pure	16	18.701 ±2.49	76.05 ±3.42	4.863 ±0.74
Oak/pure	16	21.104 ±1.67	83.17 ±3.21	5.272 ±0.86
Pine/mixed	16	19.981 ±1.76	84.20 ±4.88	6.080 ±1.17
Oak/mixed	16	20.121 ±1.38	82.06 ±2.82	5.461 ±1.08

Comment 32. Figure 3 – please italics the species names

Authors: *Revised and corrected*

Comment 33. Figure 4 – looks like you have some attenuation of the signal (e.g., where label “a” is located). Also what do the lowercase letters represent?

Authors: *The reviewer is correct, in the last two radargrams of figure 4 it is shown an attenuation in the hyperbolic reflectances, afterwrda to have applied the Bandpass filtering routine. This radargram has been largely eliminated from the noise generated by the needles present at the site. It should be noted that these radargrams were performed using the 800 MHz GPR antenna (shown in the figures, from the response of comment 28).*

References:

Aditama, I. F., Widodo, Setiawan, T., Bijaksana, S., and Sanny, T. A.: Use of electrical geophysical methods for supporting agricultural practices, AIP Conference Proceedings, 1861, 030027, 10.1063/1.4990914, 2017.

Butnor, J. R., Barton, C., Day, F. P., Johnsen, K. H., Mucciardi, A. N., Schroeder, R., and Stover, D. B.: Using Ground-Penetrating Radar to Detect Tree Roots and Estimate Biomass, in: Measuring Roots: An Updated Approach, edited by: Mancuso, S., Springer Berlin Heidelberg, Berlin, Heidelberg, 213-245, 2012.

Kutschera, L., and Lichtenegger, E.: Wurzelatlas mitteleuropäischer Waldbäume und Sträucher, Stocker, 2002.

McDowell, F. W., and Keizer, R. P.: Timing of mid-Tertiary volcanism in the Sierra Madre Occidental between Durango City and Mazatlan, Mexico, Geol Soc Am Bull, 88, 1479-1487, 10.1130/0016-7606(1977)88<1479:tomvit>2.0.co;2, 1977.

Rodriguez-Robles, U., Arredondo, J. T., Huber-Sannwald, E., and Vargas, R.: Geoecohydrological mechanisms couple soil and leaf water dynamics and facilitate species coexistence in shallow soils of a tropical semiarid mixed forest, The New phytologist, 207, 59-69, 10.1111/nph.13344, 2015.

Application of geophysical tools for tree root studies in forest ecosystems in complex soils

Ulises Rodríguez-Robles[1], Tulio Arredondo[1], Elisabeth Huber-Sannwald[1], José Alfredo Ramos-Leal[2], Enrico A. Yépez[3]

[1]División de Ciencias Ambientales, Instituto Potosino de Investigación Científica y Tecnológica, Camino a la Presa de San José # 2055, Lomas 4ta Sección, C.P. 78216 San Luis Potosí, S.L.P., México.
[2]División de Geociencias Aplicadas, Instituto Potosino de Investigación Científica y Tecnológica, Camino a la Presa de San José # 2055, Lomas 4ta Sección, C.P. 78216 San Luis Potosí, S.L.P., México.
[3]Departamento de Ciencias del Agua y Medio Ambiente, Instituto Tecnológico de Sonora, 5 de Febrero 818 Sur, Col. Centro, C.P. 8500 Ciudad Obregón, México.

Correspondence to: J. Tulio Arredondo (tulio@ipicyt.edu.mx)

Abstract. While semiarid forests frequently colonize rocky substrates, knowledge is scarce on how roots garner resources in these extreme habitats. The Sierra San Miguelito Volcanic Complex in Central Mexico exhibits shallow soils and impermeable rhyolitic-rock outcrops, which impede water movement and root placement beyond the soil matrix. However, rock fractures, exfoliated rocks, and soil pockets potentially permit downward water percolation and root growth. With ground penetrating radar (GPR) and electrical resistivity tomography (ERT), two geophysical methods advocated by Jayawickreme et al. 2014 to advance root ecology, we studied root and water distribution in shallow-rocky-soils and rock fractures in a semiarid forest. We calibrated geophysical images with in-situ root measurements, and then extrapolated root distribution over larger areas. With GPR, we identified both fine and coarse pine and oak roots from 6 to 75 mm diameter at different depths into soil and fractures; besides, trees anchored their trunks using coarse roots underneath rock outcroppings. With ERT, we tracked monthly changes in humidity at the soil/bedrock interface, which clearly explained spatial root distribution of both tree species. Geophysical methods have enormous potential in elucidating root ecology. More interdisciplinary research could advance our understanding in belowground ecological niche functions and their role in forest ecohydrology and productivity.

1 Introduction

Strategies of plant water use and mechanisms of water transport at the soil–plant–atmosphere continuum are critical to understand ecosystem functioning in arid and semiarid regions, where plant productivity is primarily limited by water availability (Prieto et al., 2012;Burgess and Bleby, 2006;Li et al., 2007). Roots' major functions are absorbing water and mineral nutrients, as well as supporting stems and anchoring plants to the ground (Prieto et al., 2012). Growing roots change soil structure, displace pore water and gas, and increase porosity (Jackson et al., 1996). Plant water balance and physiological processes depend on the control of root water uptake (Anderegg and HilleRisLambers, 2016). Placement of roots at different soil depths favor both spatial and temporal resource partitioning and effective resource exploitation of whole soil profiles, thereby enhancing biomass production (Fernandez et al., 2000;Brooks et al., 2002;Hultine et al., 2003;Renee et al., 2010). Many ecosystems with shallow soils (<1 m) are located in water-limited climatic regions with highly variable, seasonal precipitation, where a small water storage potential in the substrate is paramount to maintain perennial vegetation cover (Rose et al., 2003;Schwinning, 2010;Rodriguez-Robles et al., 2015). So far, there exist a fair number of studies on hydrological aspects of plants from semiarid regions, in particular, from sites where vertical root development is not restricted by hardened soil layers such as in karstic regions (Schwinning and Ehleringer, 2001;Poulos et al., 2007;Lebourgeois et al., 1998;Estrada-Medina et al., 2013). Few studies, however have examined semiarid forest ecosystems with shallow soils forming over bedrock, cemented horizons, or strongly developed argillic horizons that impede downward water movement and root growth (Andrews et al., 2005;Katra et al., 2008;Rodriguez-Robles et al., 2015).

In semiarid climates, poorly developed shallow soils over water-impermeable substrates rarely exhibit sufficient water storage capacity to maintain forest ecosystems. Empirical evidence suggests that trees and shrubs growing on this type of substrate are able to access water from weathered bedrock once water supply from the top soil becomes exhausted (Schwinning, 2008;Querejeta et al., 2007). Still, the geological context of shallow soils in plant-water relations is controversial both in terms of the physical source of water and the adaptive mechanisms to thrive under these limiting water conditions. This has been the focus of recent ecohydrological studies (Tokumoto et al., 2014;Schwinning, 2013;Rodriguez-Robles et al., 2015;Estrada-Medina et al., 2013). Because of methodological difficulties, the impracticality of bedrock excavation and a general lack of specific research tools to study root distribution *in-situ*, little is known about species-specific rooting patterns and growth strategies of forest ecosystems colonizing shallow soils over bedrock. Complementary methods are needed to simultaneously study vertical root distribution and seasonal soil humidity patterns to elucidate potentially diverse species-specific adaptations to complex geoecohydrological conditions.

With surface geophysical methods, such as electrical resistivity tomography (ERT), it is possible to monitor water content at soil-bedrock depths between 2.5 and 17 m and at frequent time intervals (Beff et al., 2013). ERT is a nondestructive, geoelectrical method to examine soil properties (Martinez-Pagan et al., 2013); it allows the generation of two- and/or three-dimensional images and maps depicting both the spatial and temporal variation in soil electrical conductivity, corresponding to variations in soil water content (Cosentini et al., 2012), and singularities like cracks and fractures (Travelletti et al., 2012). The resistivity of rocks and soil may vary depending on their water content, water salinity and mode of pore distribution, with a wide range of values ($1\text{-}10^9\ \Omega\cdot m^{-1}$); lower values indicate higher water content and vice versa (Orellana and Silva, 1982). ERT has traditionally been used in geological prospecting (Chrétien et al., 2014;Sudha et al., 2009;Wang et al., 1991), but it is now also frequently applied in hydrological, agricultural and environmental studies (Srayeddin and Doussan, 2009;Jackson et al., 2000).

Ground-penetrating radar (GPR) is an effective and rapid tool for geophysical surveys because it is non-destructive and delivers real-time information (Parsekian et al., 2015). The GPR permits the use of a variety of antennas with different (high and low resolution) frequencies for the examination of different substrates and to be used by multiple disciplines. The ground electrical conductivity, the transmitted center frequency, and the radiated power, all may limit the effective depth range of GPR prospection. Increases in electrical conductivity in the ground may attenuate the introduced electromagnetic wave, and thus its penetration depth decreases. However, higher GPR frequencies may provide improved resolution. Hence, operating frequency is always a trade-off between resolution and ground penetration (Aditama et al., 2017). The application of GPR ranges from characterizing subsurface stratigraphy (Adepelumi and Fayemi, 2012) and spatial extent of weathered blocks and fracture-cracked systems (Ogretmen and Seren, 2014) to measurements of soil water content (da Silva et al., 2004) and the determination of belowground tree roots of different diameter (with minimum diameter of 5 mm) in forest and urban settings (Tanikawa et al., 2013;Ow and Sim, 2012;Hruska et al., 1999). A combined application of GPR with ERT explored the distinction and distribution of roots with different diameters over a broad range of soil conditions in south-eastern United States (Butnor et al., 2001). According to their study, soils with high electrical resistivity are the most amenable for root detection with GPR. More recent studies (Zhu et al., 2014;Borden et al., 2014) have tried to track the direction (vertical or horizontal) of root growth and to evaluate the efficiency of GPR in mapping coarse root systems and estimating root biomass under field conditions. However, various factors affect detection of roots using GPR, such as root position, wood density and the conditions surrounding roots. These conditions include for instance, physical properties, altered or removed material, the volumetric water content, temperature, dissolved solids or salinity, the existence of regolitic material, and applied GPR wave frequency. These conditions may interfere with signal transmission and thus resulting in low-quality and difficult-to-interpret profiles (Table 1). For example, root zones in wet conductive soils, high-frequency waves are strongly attenuated limiting the resolution to detect roots and depth penetration (Butnor et al., 2012).

To explore the potential of these geophysical methods in ecology, we examined ecohydrological processes at the soil-bedrock-plant root interface in a mixed forest ecosystem in the mountainous region of Sierra San Miguelito (SSM) situated at the transition of the arid desert scrub biome in the North and the semiarid grassland biome in the South of the Mexican Central Plateau. Since the presence and success of pine-oak forests in this macroclimatic semiarid region cannot be explained by mere climate conditions, we used geophysical methods to elucidate the geological and edaphic conditions as well as potential root adaptations, to help explain the ecohydrological functioning of this azonal forest. The SSM is a volcanic complex of impermeable rhyolitic rocks, whose surface layers have been highly weathered by exfoliation processes (peeling off in sheets). The forest ecosystems are characterized by shallow, poorly developed soils with high litter and organic matter content (<25 cm deep) (Perez et al., 2009). Recent studies suggested that native tree species may be able to extract water directly from subsurface bedrock (Schwinning, 2013;Proust et al., 2011;Tokumoto et al., 2014), however, most of these studies have focused on water-permeable rock types (e.g., limestones). Rodriguez-Robles et al. (2015) suggested that specialized root systems of tree colonizing the shallow rocky soils of SSM explore large regolith rocky areas and thereby increase the likelihood of finding stored water in cracks. However, it is unclear if the water supply encountered in cracks fulfills the water demand of two coexisting tree species especially during frequently recurring extended seasonal droughts in this region. Also, little is known about the distribution of fine and coarse tree roots growing below shallow soils into weathered bedrock, mainly because of difficulties in excavating bedrock. Overall *Quercus* species exhibit dimorphic roots, while *Pinus* species display preferently superficial roots spreading horizontally (Kutschera and Lichtenegger, 2002).

This study responds to a cross-disciplinary call for the application and wide use of new geophysical methods to advance *in-situ* research in root ecology (Jayawickreme et al., 2014). Our study adopted a novel approach to tackle several questions simultaneously and by drawing upon diverse disciplines such as ecosystem ecology, ecohydrology, geophysics, and biogeosciences. Here, we present details on the application of surface geophysical imaging tools for root research studies in mixed forests in an edaphically, geologically and climatically extreme and complex environment. We emphasize the application of these tools primarily for exploration and thus as an alternative and/or complement to traditional ecological methods to gather information on ecologically relevant subsurface variables across time and space. We expected weathered rhyolite bedrock in Sierra San Miguelito Volcanic Complex (SSMVC) to conserve humid microsites and that the root distribution of pine-oak forest stands mirrors spatial and temporal heterogeneity of water availability. In particular, we aimed at: (1) characterizing the presence and depth of weathered bedrock and demonstrating that exfoliation sites function as potential water sources; (2) with the use of GPR, detecting roots of different diameter size classes growing at various depths in volcanic fractured rock; (3) with the use of ERT, assessing the relationship between soil electrical resistivity and soil water potential in order to determine if resistivity tomography can detect the spatial and temporal variability of soil moisture beneath vegetation patches; and (4) with ERT tomograms and GPR radargrms, describing the functionality of weathered bedrock in forest ecosystems colonizing shallow rocky soils.

2 Materials and methods

2.1 Site description

The site is situated in SSM, in a semiarid pine-oak forest ecosystem in the Southern region of the SSMVC (Fig. S1). The SSMVC represents the remnants of one of the most voluminous rhyolitic volcanic events on Earth (McDowell and Keizer, 1977), formed by massive lava spills of rhyolitic composition (Portezuelo Latite and San Miguelito Rhyolite). Currently, this volcanic complex is affected by small-scale local fracturing through pedogenesis and hydrological processes and thereby is directly influencing pine-oak forest establishment (Fig. 1a-b). Soils are poorly developed and overall extremely shallow (<25 cm) and rocky; hence, to get support, tree roots commonly anchor in weathered bedrock or beneath rock outcrops (Fig. 1c-d). Lithological profiles show a high density of vertical roots in rock fractures and soil pockets (Fig. 1e-f). According to the World Reference Base for Soil Resources (WRB) classification system, the soil at this site corresponds to lithic-paralithic Leptosols (LPlip) (FAO, 2006). Organic matter content is very high (60%) in these soils (Perez et al., 2009). The climate is semiarid; for the last 65 years mean annual precipitation (MAP) has averaged 408 mm (weather station “La Purisima”, 22° 5' 22.4", 101° 12' 28.9"), where in 64% of the years MAP has been below average and only in 12% MAP has been above 500 mm (Fig. S2). In general, summer precipitation falls between July and October and accounts for 90% of MAP, the rest falls between December and February.

2.2 Experimental plots

Along a 2.5 km long transect running parallel to a narrow watershed, where pine and oak trees are evenly distributed in pure and mixed stands, we established a total of 12 circular experimental plots of 25 m diameter with four replicates per stand type (pine, oak, and mixed stands). In addition, for the exploration and tracking of roots with the GPR, we established one 8.5 x 6 m plot with parallel transects (spaced 1 meter) to observe horizontal axis elongation of roots in a mixed stand and one concentric plot of five circular transects around an anchored *Pinus cembroides* tree (with 0.1, 0.3, 0.5, 1.0, and 1.5 m distance between neighboring transects). To monitor soil water potential (Ψ_s) at biweekly intervals, in September 2013, each circular plot was equipped with four (64 total) soil psychrometer sensors (PST-55, Wescor Inc. USA), which were inserted at 12 to 15 cm depth (depending on the depth of soil pockets) near tree trunks (Table 2). To determine electric resistivity, 72 geophysical electrodes (24 for each stand type) were installed with Northeast-Southwest orientation with 1 m inter-electrode spacing (along the slope). GPR radargrams were generated using a MALÅ RAMAC X3M GPR / ProEx system coupled to an inspection wheel. Electric Resistivity Tomography (ERT) tomograms were taken using the SYSCAL KID SWITCH-24 (IRIS instruments) with a 24-multi-electrode switch box.

2.3 Principles of GPR

GPR is an impulse radar system designed for shallow subsurface investigations from 1 to 25 m depth. A transmitting antenna of a certain frequency sends electromagnetic pulses from the soil surface through the soil matrix; a boundary layer is reflected when the transmitted pulse crosses two objects of different electromagnetic properties (Van Dam, 2014). Consequently, the reflected wave returns to the receiving antenna at ground level (or soil surface), which measures the reflected signal as a function of time (Butnor et al., 2001). Reflections and diffractions of electromagnetic waves may occur at boundaries between rock strata and objects that exhibit differences in electrical properties. Most soils and rocks have extremely low conductivity (about $< 10^{-2}$S/m), thus the propagation of electromagnetic waves is mainly affected by electrical dielectric constants of soils and rocks (Heggy et al., 2003). Electric permittivity, $\mathcal{E}$, and electric conductivity, σ, are petrophysical parameters that determine the reflectivity of boundary layers and penetration depth. Generally, the reflection of an electromagnetic wave occurs at boundary layers and its strength is shown by the reflection coefficient, r, which is determined by (Blindow et al., 2007):

$$r = \frac{\sqrt{\varepsilon_1} - \sqrt{\varepsilon_2}}{\sqrt{\varepsilon_1} + \sqrt{\varepsilon_2}}$$

In this equation, $\mathcal{E}_1$ and $\mathcal{E}_2$ are the dielectric constants of roots and soil, respectively. Specifically, the contrast in dielectric constants between a root and the surrounding soil determines root radar reflectance (Fig. S3a). The larger r and the stronger the reflected wave at the boundary layer, the size and bow of the resulting hyperbola vary according to the amplitude of the reflected wave. The difference in dielectric permittivity of a root and its surrounding matrix forms a boundary, which then can be detected by a traveling electromagnetic wave; however, it varies in time and space as a function of soil (texture, water content) and root characteristics (size, depth, orientation, water content). When a traveling electromagnetic wave hits a boundary between materials with differing electromagnetic properties, such as dry soil and water-conducting roots, part of this wave is reflected (Raz-Yaseef et al., 2013) often producing hyperbolic patterns (Butnor et al., 2001). We have worked with waveform parameters of the time interval between zero crossings (ns) of maximum and minimum reflected waves (Guo et al., 2013).

2.4 Principles of ERT

ERT is a method that produces images of the variation of electrical resistivity in either two or three dimensions, below a line or grid of electrodes placed on the soil surface. ERT tomograms consist of a modeled cross-sectional plot of resistivity ($\Omega\cdot m^{-1}$) versus depth. The method is based on measurements of voltage differences between electrodes. This is a minimally invasive method, because it only requires inserting electrodes a few centimeters into the ground to create electrical contact. The resulting subsurface resistivity model depicts variations in the conductivity of electrical current in subsurface soils and rocks (Fig. S3b). Resistivity is the mathematical inverse of conductivity. The measured resistivity is a function of water content of the substrate (rock or soil), the chemical composition of pore water and the soil surface area/grain particle size distribution. The relations of these variables are summarized in Archie's law, an empirical equation of resistivity, ρ [$\Omega\cdot m^{-1}$], of rocks (König et al., 2007):

$$\rho = \frac{a}{\phi^m S^n}\rho_w$$

where Φ (porosity) and S (saturation factor) are fractions between 0 and 1, ρ_w [$\Omega\cdot m^{-1}$] is the resistivity of groundwater, and the parameters a (tortuosity), m (cementation factor), and n (saturation exponent) are empirical constants that need to be determined for each study area.

2.5 Data collection

From October to December 2012, we examined the frequency, size, position and depth range of roots with 2.5 to 7.5 cm diameter in the top soil and under exfoliated rocks, using the GPR 500 MHz antenna and working with a 2.5 m depth window. To characterize the exfoliation of weathered bedrock soil, and to differentiate between the exfoliated rock base and potential root axes (0.6 to 4 cm diameter) underneath rocks, we used the GPR 800 MHz antenna, exploring at 1 m depth. Root identification in radargrams was a stepwise process; first, roots were recognized at locations where hyperbolas of reflected waves had relatively higher amplitudes compared to those in the surrounding area (Cui et al., 2011). Then, to determine the diameter and depth of these roots, the time interval between zero crossings (ns, time interval for maximum reflected wave) was extracted at the points of hyperbolas, where roots had been identified previously. The detection frequency for the number of roots identified in the radar profile was calculated along each transect for five root diameter classes (< 3.0, 3.0 – 4.0, 4.0 – 5.0, 5.0 – 6.0, and > 6.0 cm). Finally, for calibration purposes, individual roots (total of 76) were excavated to determine their depth and diameter *in-situ* (Table 3, Fig. 2a).

Based on the assumption that electrical resistivity decreases with increasing water content (Nijland et al., 2010;Jayawickreme et al., 2014), we compared the spatial and temporal patterns of soil and bedrock moisture within and among forest stands. During an 8-months period, we generated 12 ERT tomograms (four for each stand type) during wet (October 2013 and February 2014) and dry (December 2013 and May 2014) ecohydrological periods. Here we present one representative profile for each forest stand. To relate Ψ_s data with ERT surveys, Ψ_s was measured at diurnal peaks of water stress (from 11 to 14 hrs) every two weeks during an 8-months period (October 2013 to May 2014).

Finally, to trace short-term percolation responses and the progress of water profiles (March 2013) during the dry season, 15 liters of water were injected into a shallow fracture of 35 cm length in an oak stand; 150 minutes later, we generated radar profiles along a 3.3 m transect running parallel to the slope with the 800 MHz antenna.

2.6 Data processing and Interpretation

In field the following settings were used: time windows (400 ns), stacks (auto), sampling fewquency (1120 MHz), point distance (0.001 m) and velocity (110 m/µs). Raw GPR radargrams were processed with RadExplorer v1.42 software (Mala GeoScience, USA Inc) prior to interpretation Post-acquisition processing of radar data is accomplished to reduce clutter, minimize the effects of multiple hyperbolic reflections and enhance the signal-to-noise ratio (Daniels, 1996). Filtering of radar data removed unwanted signals (noise) and corrected the position of reflectors on the radar record. The sequence of filter application depends on the accuracy of collected radargrams and the study's objective. Radar signals are tend to attenuation and loss with increasing depth during the propagation of soil. The greater the signal loss is at deeper detection area. Thus, the signal data require dependent gain which compensates for amplitude reduction with depth (star point: 30). Prior to compensate for gain, in order to ensure that the mean of data is zero, the GPR data must remove the DC component, from the monitor (ProEx system - Adjust signal position). Signal gain processing requires data with less noise, or the noise may be magnified. For each particular case, radargram processing follows specific procedures: data editing, correction of time zero, background removal filter, Bandpass filtering and Stolt F-K migration (Butnor et al., 2012). In this study, for root exploration all radargrams were processed with the same range of filter values, because the whole study area had similar characteristics with a horizon of organic soil and weathered bedrock underneath.

- The *correction of time zero*, the start time that may not be detected precisely by the system is corrected here to match with surface position and ensure correct depths in the profile. not be detected precisely by the system is corrected here to match with surface position and ensure correct depths in the profile.
- The *background removal filter* eliminates parallel bands resulting from plane reflectors such as ground surface, leaf litter, soil horizons (when it comes to identifying roots in the soil), and bands of low-frequency noise.

- We have largely removed noise by vertical high-pass filter and vertical low-pass filter (*Bandpass filtering* : 700 – 1400 MHz) (Butnor et al., 2003;Dahboosh Al-Shiejiri, 2013).
- *Stolt F-K migration* routine was used to correct for object position and collapsed hyperbolic reflections (diffracted waves) based on signal geometry (migration velocity: 12.8 cm/ns) (Doolittle and Butnor, 2009).
- The waveform parameter of the time interval between zero crossings (ns) of the maximum reflected wave was extracted at the points of root detection in the radar profiles and calculated using RadExplorer v1.42 software.

Electrical resistivity tomography was conducted using a wenner-switch array. Resistivity values were corrected for the effect of temperature, based on the temperature recorded by the closest soil psychrometer sensor at a given depth for each resistivity value, and on the Campbell equation (Campbell et al., 1949) as suggested by Samouëlian et al. (2005):

$$\rho = \rho T[1 + \alpha(T - 25)]$$

where,

T corresponds to temperature (◦C), ρT is the electrical resistivity measured at temperature T ($\Omega\cdot m^{-1}$), ρ is the electrical resistivity at the reference temperature of 25 ◦C ($\Omega\cdot m^{-1}$), and α refers to a correction factor equal to 0.0202.

Inversion and forward simulations were performed with RES2DINV software (Geotomo software) for later manipulation of data files with the ArcMap module applying an Empirical Bayesian Kriging method (ArcGIS Desktop, ESRI 2011). For more details on the softwares and algorithms used see Krivoruchko, 2012 and Loke, 2015.

2.7 Statistical analysis

Nested two-way analysis of variance was used to examine differences in root diameter. The model included two factors, forest stand with three levels (pure and mixed pine and oak stands; fixed effect) and soil depth with four levels (10, 20, 30 and >30 cm; nested effect); in case of significant interactions we conducted Tukey's *post hoc* mean comparison test. We ran Type I regression analyses to examine the relationships between root diameter and time interval between zero crossings (ns) for both frequency antennas to calibrate the method. Polynomial quadratic regression analyses were conducted to examine the relationship between Ψ_{soil} (MPa) and resistivity ($\Omega\cdot m^{-1}$). Prior to statistical analysis we applied Shapiro Wilk's test to examine normality of the residuals. All statistical analyses were run in SAS University Edition (Free Statistical Software).

3 Results

All geophysical images helped interpret the spatial distribution of tree roots in soils and weathered bedrock, as well as of rocky soil characteristics. However, some difficulties in the interpretation of raw radargrams (unfiltered radar profiles) included noise and ghost areas caused by characteristics of organic and rocky soils. Nevertheless, radargrams indicated clear hyperbolic reflections that corresponded to the position of tree roots at certain depths (Fig. S3a). ETR tomogram results (Fig.

S3b) for the top 50 cm helped identify areas of greatest drainage (200-450Ω·m^{-1}) and fracturation (400-700Ω·m^{-1}). ETR tomogram outputs of RES2DINV software did not reveal the exfoliated rock that occur in the study area.

3.1 GPR detection of tree roots and diameter estimation

We examined the relationships between root diameter and time interval between zero crossings (ns) using 500 MHz signals ($P < 0.0001$, $R^2 = 0.93$, Table 4, Fig. 2a). With this antenna, we detected roots as fine as 2.5 cm diameter and as coarse as 7.5 cm in different tree stands. In pure pine stands, the finest roots (2.5-3 cm) were preferentially located in the top 10 cm of the organic soil, while coarse diameter roots occurred mostly at 30 cm depth (Table 5, Fig. 2b). In contrast, in pure oak stands root diameter decreased with increasing soil depth (Fig. 2b). Also, in mixed stands, deeper roots had overall smaller diameters (Fig. 2b) than roots in shallow soils. It is important to remark that in pure pine stands no roots occurred below 30 cm depth. Fig. S4, depicts a typical radargram generated with a 500 MHz antenna after having applied band pass filtering and the background removal filter. The GPR radargram of a mixed forest stand revealed the highest aggregation of coarse roots near the tree bases and their adjacent areas, as well as a high heterogeneity of root diameter distribution between trees (Fig. S4). Radargrams also revealed a clear boundary layer between the soil and the rocky substrate (Fig. S4: continuous line) and soil pockets (Fig. S4, dotted line). These soil profiles were validated *in situ*.

In a mixed stand, a two-dimensional radargram sequence was generated with the 500 MHz antenna in a 8.5m x 6m horizontal tracking quadrant; both pine and oak roots (different uppercase letters in Fig. 3) were validated *in-situ*. For this serial root mapping consisting of 7 sequential radargrams, we identified a total of 386 roots in their horizontal position. Diameters of single roots were highly variable (2.5-6 cm), as well as signal outputs (hyperbolas) for deep roots (5-30 cm). With this sequential series of radargrams, we could track the horizontal distribution of single root axes (for instance root "B" in the different radargrams) (Fig. 3b - g). We found high variation in root diameters along a 6 m transect (root diameters in radar profile a = 6.5, b = 4.8, c = 5.2, d = 5.8, e = 6.4, f = 4.6, g = 3.8 cm) in accordance with the size of signal amplitude (in radar profile a = 1.16, b = 0.78, c = 0.84, d = 0.94, e = 1.09, f = 0.73, g = 0.61 ns). Roots with larger diameters had higher signal amplitudes, whereas smaller diameter roots had lower amplitudes.

We identified pine trees anchored under exfoliated rocks by applying 800 MHz antenna along concentric transects around a tree and after adopting background removal routines (Fig. 4). We observed a significant relationship between root diameter and time interval between zero crossings using 800 MHz signals ($P < 0.0001$, $R^2 = 0.97$, Table 4, Fig. 2a). The radargram also revealed (Fig. 4b, uppercase letters) roots under exfoliated rocks, which were then used to calibrate the radargram. This technique allowed us to differentiate between the base of exfoliated rocks (about 35 cm deep) and the presence of thin roots underneath that bedrock (0.6 to 4 cm in diameter). In the transect at 50 cm distance from the trunk, three hyperbolas were reflected, suggesting root presence under the exfoliated rocks (Fig. 4b). By increasing transect length, the number of reflected hyperbolas increased under the bedrock (e.g., transect at 100 cm distance from tree base) and the rock limits, permitting to track root elongation in shallow rocky soils. Also, it was possible to match a high signal amplitude with a pine tree anchored beneath an exfoliated rock (Fig. 4b, letter "B") and its associated lateral roots (Fig. 4b, arrows). In spite of filtering routines, it is impossible to completely remove all noise sources in all radargrams; e.g., there was some residual noise associated with leaf litter accumulation under and on top of exfoliated rocks, however *in situ* verification confirmed that radargrams spotted primarily tree roots.

3.2 Distribution of roots and subsurface resistivity imaging

ERT tomograms of different forest stands revealed a clear horizontally layered structural organization of weathered rock with exfoliation (Fig. 5). The tomograms at 0-2 m depth showed a wide range of resistivity values with maxima >1000 $\Omega \cdot m^{-1}$ observed at tomogram bottoms and a minimum between 250 and 650 $\Omega \cdot m^{-1}$ at the surface horizons. In the upper horizons (< 0.5 m), the observed low resistivities (< 450 $\Omega \cdot m^{-1}$) corresponded to islands of higher root densities beneath vegetation patches and were associated with water extraction zones; high resistivities (> 450 $\Omega \cdot m^{-1}$) coincided with bedrock outcroppings. Considering vertical distributions of pine and oak roots (Fig. S4), ERT tomograms clearly matched root distribution to species-specific vegetation cover at the measurement points.

Following seasonal drought (Dec 2013 to May 2014), ERT profiles of all stands exhibited increasing resistivity between 0 and 1 m depth (Fig. S5), which was likely attributed to soil drying as a consequence of both root water uptake and soil evaporation. Thus, in the top meter, we observed the largest spatial variation in bedrock moisture content ranging from 250 - 1450 $\Omega \cdot m^{-1}$ (Ψs = -0.5 to -24.5 MPa). By visual assessment, both mixed and pure oak stands showed highest moisture content in all four monitored periods (Fig. S5e - l). Pure pine stands preferentially occurred on sites with deepest soils (up to 60 cm), while pure oak stands anchored mostly on exfoliated rocks. Mixed stands had a combination of both abiotic site characteristics.

Soil resistivity and soil water potential were negatively related considering all observations from the different stands ($R^2 = 0.95$; $P < 0.0001$, Fig. S6). Thus, as resistivity increased Ψs dropped; this trend was apparent for resistivity values up to around 750 $\Omega \cdot m^{-1}$ being proportional to almost -6 MPa.

3.3 Fracturing as a secondary water supply to forest trees

In the dry season, upon water injection into a rock fracture next to an oak tree base growing on exfoliated rock (Fig. 6a), we observed a response signal in form of a wave amplitude equivalent to those observed underneath vegetation patches (Fig. 6b). Radargrams showed a clear infiltration horizon at approximately 50 cm depth. The signal appeared 150 minutes after water injection; while it was not homogeneous for all vegetation patches, because of different root densities and other microsite differences, we could detect a remarkably rapid horizontal displacement of water up to three meters distance from where it was injected.

4 Discussion

In semiarid environments, forest ecosystems that develop on young volcanic bedrock and poorly developed soils face two independent growth limitations, 1) highly variable precipitation as well as increasing frequency of droughts, and 2) extremely low water storage capacity of soils. Hence, insight into the distribution of different tree root types at the soil-bedrock interface and the spatio-temporal availability of water is fundamental for understanding tree ecophysiology, tree population dynamics, tree species interactions, and forest ecosystem functioning. Lack of instruments and technology to study belowground root ecology has delayed scientific advances in forest ecosystem ecology in semiarid regions. However, with interdisciplinary efforts and the employment of geophysical tools and standard methods in ecosystem science (e.g., use of natural abundance and tracer stable isotopes) potentially great advances may be achieved in our understanding of the underlying geoecohydrological mechanisms that may explain tree species coexistence in extreme water-limiting environments (Rodriguez-Robles et al., 2015). Here, we demonstrate the enormous potential of applying geophysical tools to examine non-destructively and in real-time soil-bedrock-water and root characteristics.

With the use of GPR, we clearly detected pine and oak roots with diameters ranging between 0.6 and 7.5 cm under natural soil conditions (root diameters of 2.5 to 7 cm and 0.6 – 4 cm with the 500 MHz and 800 MHz antenna, respectively; Figs. 2 and S4). Typically belowground studies using GPR are carried out in sites with homogeneous soils, such as forest plantations, gardens, parks, backyards, crop fields, or under highly controlled conditions (Ow and Sim, 2012;Cermak et al., 2000;Cox et al., 2005;Dannoura et al., 2008;Zenone et al., 2008;Zhu et al., 2014) to reduce the difficulty in detecting and interpreting the origin of reflected signals (hyperbolic). In our case, it was fundamental to use high and low frequency antennas, as they gave valuable complementary information on these complex shallow rocky soils over volcanic bedrock. With the 500 MHz antenna, we could differentiate between and characterize a series of vertical substrate layers, whereas with the 800 MHz antenna we could locate thin roots underneath exfoliated rocks. However, with the 800 MHz antenna, detection efficiency of fine roots decreased in sites with high litter accumulation of fresh pine needles on exfoliated rocks (Fig. 4). Similar difficulties for GPR interpretation had been mentioned previously; for instance (Hirano et al., 2009) reported that soil water content may greatly limit the detection of reflected waves originating from roots. In October 2013 (a wet month), we carried out an experiment with the GPR 500 MHz to examine the wetness effect in one of the experimental plots. Under high soil moisture content, we did not get a signal from the roots at this site, most likely because the signal wavelength gets lost by undetected changes in the dielectric properties between roots and soil (material interface) (Guo et al., 2013;Hirano et al., 2012;Butnor et al., 2009). Although our GPR survey was carried out in the dry period, we were still facing some difficulties to accurately differentiate between hyperboles deriving from different yet overlapping roots. The experiment of local water injection in a rock fracture (Fig. 6), greatly helped to clearly identify and separate the hyperbolas (roots) in the radargram.

4.1 Dynamics of water inside of weathered bedrock and spatial distribution of roots

In forests colonizing shallow soils and impermeable volcanic bedrock, water availability largely depends on the soil-weathered bedrock interaction (Fig. 5). In one particular case, water of an accumulated 87 mm rain event occurring in February, infiltrated and percolated down to only 50 cm depth (Fig. S5 c, k). Although volcanic bedrock is characterized by low permeability, rock fracturation may contribute to what can be called “secondary substrate porosity” in impermeable bedrock, thereby allowing water-flow and storage within volcanic bedrock (Carrillo-Rivera et al., 1996). The analysis of ERT tomograms revealed a clear detachment of rock layers (exfoliation) (Fig. 5) and the presence of soil pockets (Fig. 5b, located at 18.4 m of the transect), which are both formations that potentially favor water storage. These conditions appear to promote the establishment and anchorage of trees under otherwise highly limiting soil water conditions. Several studies have reported that trees can get established in rock fractures (mainly calcic and permeable bedrock) (Estrada-Medina et al., 2010;Poot and Lambers, 2008) and that they locate their roots inside of this permeable material to exploit stored water (Schwinning, 2013;Querejeta et al., 2007). The combination of tomogram and radargram images (Fig. 5) revealed distinctive microsites in this shallow layer of weathered bedrock suitable for trees establishment and the formation of vegetation patches. Also, our results suggest that oak and pine might exhibit complementary strategies to access different water sources. Oak distributes its finest roots in both the soil organic layer and in the soil-weathered bedrock interface (Figs. 2b, 5b). This rooting pattern may enable oak to access water retained in weathered bedrock during the dry periods (Fig. 6). Pine, in contrast, absorbs water exclusively from shallow surface soil (Figs. 2b, 5a). Species-specific differences and preferential horizontal (pine) and vertical (oak) root distribution in these geohydrological niches suggest the two species coexist in these ecosystems (Rodriguez-Robles et al., 2015). Additional studies are needed to attest this possibility.

Our assay of injecting water into a rock fracture in the dry period showed that oak roots responded rapidly, i.e. within 150 minutes, to a short-term water pulse, which moved 300 cm laterally, suggesting some sort of channel type connection between fractures and exfoliated rocks (Fig. 6). Hence, exfoliated rocks may play key bi-functional ecological role: they support tree anchorage (Fig. 4a) and serve as vital water entry, reservoir and distribution points during dry periods (Fig. 6b). Root anchorage in exfoliated rocks at this site can be considered as a survival strategy, since trunks and horizontal roots located below exfoliated rocks obtain physical support, which cannot be provided otherwise in these particularly shallow soils (Fig.5).

5 Conclusion

This study highlights thus far underexplored yet potentially extremely powerful tools of geophysical imaging in forest ecohydrology. They allow *in situ* non-destructive estimation of a wide range of tree root diameters, with 0.6 cm as the highest resolution of diameter and the location of short-term and long-term water reservoirs in a complex soil – rock terrain. Furthermore, non-invasive mapping of GPR and ERT provides detailed field-level information of geohydrological characteristics of the soil - weathered bedrock interface, which were traditionally assessed with coring and excavation methods. This study demonstrates that the application of ERT and GPR has an enormous potential to capture belowground spatial and temporal characteristics of roots and soil moisture distribution at the field scale.

While these tools offer many advantages for the study of belowground *in situ* aspects of ecosystems and RadExplorer and ArcGis software allow powerful image processing and manipulation of radargrams and tomograms, we want to highlight the major limitations encountered in this study; certain field conditions (e.g., leaf litter, weathered bedrock regolith) i) impede or reduce the detection potential and quantification of coarse roots when using the GPR 500 MHz antenna; ii) they also reduced the capability of the GPR 800 MHz antenna to delineate reflection signals emitted by roots; iii) an increase in soil moisture may decrease the electromagnetic gradient between roots and soil, such that reflected signals get considerably weakened, which makes root delineation more difficult under wet conditions; iv) given the contact resistance problem for electrodes in the ERT survey that result especially during dry periods, from moisture content in the soil-bedrock and soil temperature. We minimized these problems by pre-cleaning the surface of litter and twigs (points i and ii) and by applying copper sulfate gel in the inserted electrodes (point iii).

Geophysical images are highly valuable and promising tools to advance our understanding of the coupled nature of geoecohydrological patterns and processes by linking belowground geophysical structures with soil/bedrock hydrological characteristics and root ecology.

6 Author contributions

U.R.-R., J.T.A. and J.A.R.-L. planned and designed the research and executed the field experiments. U.R.-R., J.T.A., E.H.-S. and E.A.Y. analyzed the data and wrote the manuscript.

7 Acknowledgements

We thank Alejandro Cruz Rosas Palafox for technical advice in the use of the ERT equipment. We thank the Applied Geosciences Division at IPICYT for providing access to geophysical instruments and tools. URR acknowledges the National Council for Science and Technology of Mexico (CONACyT) for the scholarship no. 332356 granted to pursue his PhD degree. This work was supported by grants given to JTA from CONACYT, num. 220788 and 224368.

References

Adepelumi, A. A., and Fayemi, O.: Joint application of ground penetrating radar and electrical resistivity measurements for characterization of subsurface stratigraphy in Southwestern Nigeria, J Geophys, 9, 397-412, 10.1088/1742-2132/9/4/397, 2012.

Aditama, I. F., Widodo, Setiawan, T., Bijaksana, S., and Sanny, T. A.: Use of electrical geophysical methods for supporting agricultural practices, AIP Conference Proceedings, 1861, 030027, 10.1063/1.4990914, 2017.

Anderegg, L. D., and HilleRisLambers, J.: Drought stress limits the geographic ranges of two tree species via different physiological mechanisms, Glob Change Biol, 22, 1029-1045, 10.1111/gcb.13148, 2016.

Andrews, M. Y., Ague, J. J., and Berner, R. A.: Trees and weathering: Chemical alteration of bedrock and soils in the Yale-Myers Forest, Northeastern Connecticut, Abstr Pap Am Chem S, 229, U893-U893, 2005.

Barton, C. V. M., and Montagu, K. D.: Detection of tree roots and determination of root diameters by ground penetrating radar under optimal conditions, Tree Physiol, 24, 1323-1331, 2004.

Beff, L., Gunther, T., Vandoorne, B., Couvreur, V., and Javaux, M.: Three-dimensional monitoring of soil water content in a maize field using Electrical Resistivity Tomography, Hydrol Earth Syst Sc, 17, 595-609, 10.5194/hess-17-595-2013, 2013.

Blindow, N., Eisenburger, D., Illich, B., Petzold, H., and Richter, T.: Ground Penetrating Radar, in: Environ Geol, Springer Berlin Heidelberg, 283-335, 2007.

Borden, K., Isaac, M., Thevathasan, N., Gordon, A., and Thomas, S.: Estimating coarse root biomass with ground penetrating radar in a tree-based intercropping system, Agroforest Syst, 1-13, 10.1007/s10457-014-9722-5, 2014.

Brooks, J. R., Meinzer, F. C., Coulombe, R., and Gregg, J.: Hydraulic redistribution of soil water during summer drought in two contrasting Pacific Northwest coniferous forests, Tree Physiol, 22, 1107-1117, 2002.

Burgess, S. S. O., and Bleby, T. M.: Redistribution of soil water by lateral roots mediated by stem tissues, J. Exp. Bot., 57, 3283-3291, 10.1093/jxb/erl085, 2006.

Butnor, J. R., Doolittle, J. A., Kress, L., Cohen, S., and Johnsen, K. H.: Use of ground-penetrating radar to study tree roots in the southeastern United States, Tree Physiol, 21, 1269-1278, 2001.

Butnor, J. R., Doolittle, J. A., Johnsen, K. H., Samuelson, L., Stokes, T., and Kress, L.: Utility of ground-penetrating radar as a root biomass survey tool in forest systems, Soil Sci. Soc. Am. J., 67, 1607-1615, 2003.

Butnor, J. R., Pruyn, M. L., Shaw, D. C., Harmon, M. E., Mucciardi, A. N., and Ryan, M. G.: Detecting defects in conifers with ground penetrating radar: applications and challenges, Forest Pathol, 39, 309-322, 10.1111/j.1439-0329.2009.00590.x, 2009.

Butnor, J. R., Barton, C., Day, F. P., Johnsen, K. H., Mucciardi, A. N., Schroeder, R., and Stover, D. B.: Using Ground-Penetrating Radar to Detect Tree Roots and Estimate Biomass, in: Measuring Roots: An Updated Approach, edited by: Mancuso, S., Springer Berlin Heidelberg, Berlin, Heidelberg, 213-245, 2012.

Campbell, R. B., Bower, C. A., and Richards, L. A.: Change of electrical conductivity with temperature and the relation of osmotic pressure to electrical conductivity and ion concentration for soil extracts, 13, 66-69, 1949.

Carrillo-Rivera, J. J., Cardona, A., and Moss, D.: Importance of the vertical component of groundwater flow: a hydrogeochemical approach in the valley of San Luis Potosi, Mexico, J Hydrol, 185, 23-44, http://dx.doi.org/10.1016/S0022-1694(96)03014-4, 1996.

Cermak, J., Hruska, J., Martinkova, M., and Prax, A.: Urban tree root systems and their survival near houses analyzed using ground penetrating radar and sap flow techniques, Plant Soil, 219, 103-116, 2000.

Cosentini, R. M., Della Vecchia, G., Foti, S., and Musso, G.: Estimation of the hydraulic parameters of unsaturated samples by electrical resistivity tomography, Geotechnique, 62, 583-594, 10.1680/geot.10.P.066, 2012.

Cox, K. D., Scherm, H., and Serman, N.: Ground-penetrating radar to detect and quantify residual root fragments following peach orchard clearing, Horttechnology, 15, 600-607, 2005.

Cui, X. H., Chen, J., Shen, J. S., Cao, X., Chen, X. H., and Zhu, X. L.: Modeling tree root diameter and biomass by ground-penetrating radar, Sci China Earth Sci, 54, 711-719, 10.1007/s11430-010-4103-z, 2011.

Chrétien, M., Lataste, J. F., Fabre, R., and Denis, A.: Electrical resistivity tomography to understand clay behavior during seasonal water content variations, Eng Geol, 169, 112-123, http://dx.doi.org/10.1016/j.enggeo.2013.11.019, 2014.

da Silva, C. C. N., de Medeiros, W. E., de Sa, E. F. J., and Neto, P. X.: Resistivity and ground-penetrating radar images of fractures in a crystalline aquifer: a case study in Caicara farm - NE Brazil, J Appl Geophys, 56, 295-307, 10.1016/j.jappgeo.2004.08.001, 2004.

Dahboosh Al-Shiejiri, S. J.: Investigation of Subsidence Phenomena by GPR Technique and Geotechnical Evaluation in Baghdad City, M.SC, College of Science, Department of Geology, University of Baghdad, , 117 pp., 2013.

Daniels, D.: Subsurface penetrating radar, London, The Institution of Electrical Engineers, 320 pp., 1996.

Dannoura, M., Hirano, Y., Igarashi, T., Ishii, M., Aono, K., Yamase, K., and Kanazawa, Y.: Detection of Cryptomeria japonica roots with ground penetrating radar, Plant Biosyst, 142, 375-380, 10.1080/11263500802150951, 2008.

Doolittle, J., and Butnor, J.: Soils, peatlands and biomonitoring, in: Ground penetrating radar: theory and applications, edited by: Jol, H., Elsevier, Amsterdam, 177–192, 2009.

Estrada-Medina, H., Tuttle, W., Graham, R. C., Allen, M. F., and Jimenez-Osornio, J. J.: Identification of Underground Karst Features using Ground-Penetrating Radar in Northern Yucatan, Mexico, Vadose Zone J, 9, 653-661, 10.2136/vzj2009.0116, 2010.

Estrada-Medina, H., Graham, R., Allen, M., Jiménez-Osornio, J., and Robles-Casolco, S.: The importance of limestone bedrock and dissolution karst features on tree root distribution in northern Yucatán, México, Plant Soil, 362, 37-50, 10.1007/s11104-012-1175-x, 2013.

FAO: World Reference Base for Soil Resources, IUSS, ISRIC, FAO, Rome103, 115, 2006.

Fernandez, M., Gil, L., and Pardos, J. A.: Effects of water supply on gas exchange in Pinus pinaster Ait. provenances during their first growing season, Ann Forest Sci, 57, 9-16, 2000.

Guo, L., Chen, J., Cui, X. H., Fan, B. H., and Lin, H.: Application of ground penetrating radar for coarse root detection and quantification: a review, Plant Soil, 362, 1-23, 10.1007/s11104-012-1455-5, 2013.

Heggy, E., Paillou, P., Costard, F., Mangold, N., Ruffie, G., Demontoux, F., Grandjean, G., and Malezieux, J. M.: Local geoelectrical models of the Martian subsurface for shallow groundwater detection using sounding radars, J Geophys Res-Planet, 108, 10.1029/2002je001871, 2003.

Hirano, Y., Dannoura, M., Aono, K., Igarashi, T., Ishii, M., Yamase, K., Makita, N., and Kanazawa, Y.: Limiting factors in the detection of tree roots using ground-penetrating radar, Plant Soil, 319, 15-24, 10.1007/s11104-008-9845-4, 2009.

Hirano, Y., Yamamoto, R., Dannoura, M., Aono, K., Igarashi, T., Ishii, M., Yamase, K., Makita, N., and Kanazawa, Y.: Detection frequency of Pinus thunbergii roots by ground-penetrating radar is related to root biomass, Plant Soil, 360, 363-373, 10.1007/s11104-012-1252-1, 2012.

Hruska, J., Cermak, J., and Sustek, S.: Mapping tree root systems with ground-penetrating radar, Tree Physiol, 19, 125-130, 1999.

Hultine, K. R., Cable, W. L., Burgess, S. S. O., and Williams, D. G.: Hydraulic redistribution by deep roots of a Chihuahuan Desert phreatophyte, Tree Physiol, 23, 353-360, 2003.

Jackson, R. B., Canadell, J., Ehleringer, J. R., Mooney, H. A., Sala, O. E., and Schulze, E. D.: A global analysis of root distributions for terrestrial biomes, Oecologia, 108, 389-411, 10.1007/BF00333714, 1996.

Jackson, R. B., Sperry, J. S., and Dawson, T. E.: Root water uptake and transport: using physiological processes in global predictions, Trends Plant Sci., 5, 482-488, 10.1016/s1360-1385(00)01766-0, 2000.

Jayawickreme, D. H., Jobbagy, E. G., and Jackson, R. B.: Geophysical subsurface imaging for ecological applications, The New phytologist, 201, 1170-1175, 10.1111/nph.12619., 2014.

Katra, I., Lavee, H., and Sarah, P.: The effect of rock fragment size and position on topsoil moisture on and and semi-arid hillslopes, Catena, 72, 49-55, 10.1016/j.catena.2007.04.001, 2008.

König, F., Knödel, K., Mittenzwey, K.-H., and Weidelt, P.: Geophysical In-situ Groundwater and Soil Monitoring, in: Environ Geol, Springer Berlin Heidelberg, 475-505, 2007.

Empirical Bayesian Kriging: Implemented in ArcGIS Geostatistical Analyst: http://www.esri.com/news/arcuser/1012/files/ebk.pdf, access: 26/08/2016, 2012.

Kutschera, L., and Lichtenegger, E.: Wurzelatlas mitteleuropäischer Waldbäume und Sträucher, Stocker, 2002.

Lebourgeois, F., Levy, G., Aussenac, G., Clerc, B., and Willm, F.: Influence of soil drying on leaf water potential, photosynthesis, stomatal conductance and growth in two black pine varieties, Ann Sci Forest, 55, 287-299, 1998.

Li, S. G., Romero-Saltos, H., Tsujimura, M., Sugimoto, A., Sasaki, L., Davaa, G., and Oyunbaatar, D.: Plant water sources in the cold semiarid ecosystem of the upper Kherlen River catchment in Mongolia: A stable isotope approach, J Hydrol, 333, 109-117, 10.1016/j.jhydrol.2006.07.020, 2007.

Tutorial : 2-D and 3-D electrical imaging surveys: https://sites.ualberta.ca/~unsworth/UA-classes/223/loke_course_notes.pdf, access: 23/08/2016, 2015.

Martinez-Pagan, P., Gomez-Ortiz, D., Martin-Crespo, T., Manteca, J. I., and Rosique, M.: The electrical resistivity tomography method in the detection of shallow mining cavities. A case study on the Victoria Cave, Cartagena (SE Spain), Eng Geol, 156, 1-10, 10.1016/j.enggeo.2013.01.013, 2013.

McDowell, F. W., and Keizer, R. P.: Timing of mid-Tertiary volcanism in the Sierra Madre Occidental between Durango City and Mazatlan, Mexico, Geol Soc Am Bull, 88, 1479-1487, 10.1130/0016-7606(1977)88<1479:tomvit>2.0.co;2, 1977.

Nijland, W., van der Meijde, M., Addink, E. A., and de Jong, S. M.: Detection of soil moisture and vegetation water abstraction in a Mediterranean natural area using electrical resistivity tomography, Catena, 81, 209-216, 10.1016/j.catena.2010.03.005, 2010.

Ogretmen, Z., and Seren, A.: Investigating fracture-cracked systems with geophysical methods in Bayburt Kiratli travertine, J Geophys Eng, 11, 10.1088/1742-2132/11/6/065009, 2014.

Orellana, E., and Silva, E. O.: Prospección geoeléctrica en corriente continua, parte 1, Paraninfo, 578 pp., 1982.

Ow, L. F., and Sim, E. K.: Detection of urban tree roots with the ground penetrating radar, Plant Biosyst, 146, 288-297, 10.1080/11263504.2012.731018, 2012.

Parsekian, A. D., Singha, K., Minsley, B. J., Holbrook, W. S., and Slater, L.: Multiscale geophysical imaging of the critical zone, Rev. Geophys., 53, 1-26, 10.1002/2014rg000465, 2015.

Perez, S. M., Arredondo, M. J. T., Huber, S. E., and Vargas, H. J. J.: Production and quality of senesced and green litterfall in a pine-oak forest in central-northwest Mexico, Forest Ecol Manag, 258, 1307-1315, 10.1016/j.foreco.2009.06.031, 2009.

Poot, P., and Lambers, H.: Shallow-soil endemics: adaptive advantages and constraints of a specialized root-system morphology, The New phytologist, 178, 371-381, 10.1111/j.1469-8137.2007.02370.x, 2008.

Poulos, H. M., Goodale, U. M., and Berlyn, G. P.: Drought response of two Mexican oak species, Quercus laceyi and Q-sideroxyla (Fagaceae), in relation to elevational position, Am. J. Bot., 94, 809-818, 10.3732/ajb.94.5.809, 2007.

Prieto, I., Armas, C., and Pugnaire, F. I.: Hydraulic lift promotes selective root foraging in nutrient-rich soil patches, Funct. Plant Biol., 39, 804-812, http://dx.doi.org/10.1071/FP12070, 2012.

Proust, D., Caillaud, J., Fontaine, C., Fialin, M., Courbe, C., and Dauger, N.: Fissure and mineral weathering impacts on heavy metal distribution in sludge-amended soil, Plant Soil, 346, 29-44, 10.1007/s11104-011-0791-1, 2011.

Querejeta, J., Estrada-Medina, H., Allen, M., and Jiménez-Osornio, J.: Water source partitioning among trees growing on shallow karst soils in a seasonally dry tropical climate, Oecologia, 152, 26-36, 2007.

Raz-Yaseef, N., Koteen, L., and Baldocchi, D. D.: Coarse root distribution of a semi-arid oak savanna estimated with ground penetrating radar, J Geophys Res-Biogeo, 118, 135-147, 10.1029/2012jg002160, 2013.

Renee, B. J., Barnard, H. R., Coulombe, R., and McDonnell, J. J.: Ecohydrologic separation of water between trees and streams in a Mediterranean climate, Nat Geosci, 3, 100-104, http://www.nature.com/ngeo/journal/v3/n2/suppinfo/ngeo722_S1.html, 2010.

Rodriguez-Robles, U., Arredondo, J. T., Huber-Sannwald, E., and Vargas, R.: Geoecohydrological mechanisms couple soil and leaf water dynamics and facilitate species coexistence in shallow soils of a tropical semiarid mixed forest, The New phytologist, 207, 59-69, 10.1111/nph.13344, 2015.

Rose, K. L., Graham, R. C., and Parker, D. R.: Water source utilization by Pinus jeffreyi and Arctostaphylos patula on thin soils over bedrock, Oecologia, 134, 46-54, 10.1007/s00442-002-1084-4, 2003.

Samouëlian, A., Cousin, I., Tabbagh, A., Bruand, A., and Richard, G.: Electrical resistivity survey in soil science: a review, Soil Till Res, 83, 173-193, http://dx.doi.org/10.1016/j.still.2004.10.004, 2005.

Schwinning, S., and Ehleringer, J. R.: Water use trade-offs and optimal adaptations to pulse-driven arid ecosystems, J. Ecol., 89, 464-480, 10.1046/j.1365-2745.2001.00576.x, 2001.

Schwinning, S.: The water relations of two evergreen tree species in a karst savanna, Oecologia, 158, 373-383, 10.1007/s00442-008-1147-2, 2008.

Schwinning, S.: The ecohydrology of roots in rocks, Ecohydrology, 3, 238-245, 10.1002/eco.134, 2010.

Schwinning, S.: Do we need new rhizosphere models for rock-dominated landscapes?, Plant Soil, 362, 25-31, 10.1007/s11104-012-1482-2, 2013.

Srayeddin, I., and Doussan, C.: Estimation of the spatial variability of root water uptake of maize and sorghum at the field scale by electrical resistivity tomography, Plant Soil, 319, 185-207, 10.1007/s11104-008-9860-5, 2009.

Sudha, K., Israil, M., Mittal, S., and Rai, J.: Soil characterization using electrical resistivity tomography and geotechnical investigations, J Appl Geophys, 67, 74-79, http://dx.doi.org/10.1016/j.jappgeo.2008.09.012, 2009.

Tanikawa, T., Hirano, Y., Dannoura, M., Yamase, K., Aono, K., Ishii, M., Igarashi, T., Ikeno, H., and Kanazawa, Y.: Root orientation can affect detection accuracy of ground-penetrating radar, Plant Soil, 373, 317-327, 10.1007/s11104-013-1798-6, 2013.

Tokumoto, I., Heilman, J. L., Schwinning, S., McInnes, K. J., Litvak, M. E., Morgan, C. L. S., and Kamps, R. H.: Small-scale variability in water storage and plant available water in shallow, rocky soils, Plant Soil, 385, 193-204, 10.1007/s11104-014-2224-4, 2014.

Travelletti, J., Sailhac, P., Malet, J. P., Grandjean, G., and Ponton, J.: Hydrological response of weathered clay-shale slopes: water infiltration monitoring with time-lapse electrical resistivity tomography, Hydrol Process, 26, 2106-2119, 10.1002/hyp.7983, 2012.

Van Dam, R. L.: Calibration Functions for Estimating Soil Moisture from GPR Dielectric Constant Measurements, Commun Soil Sci Plan, 45, 392-413, 10.1080/00103624.2013.854805, 2014.

Wang, T., Stodt, J. A., Stierman, D. J., and Murdoch, L. C.: Borehole Geophysics Mapping hydraulic fractures using a borehole-to-surface electrical resistivity method, Geoexploration, 28, 349-369, http://dx.doi.org/10.1016/0016-7142(91)90041-A, 1991.

Yan, H., Dong, X., Feng, G., Zhang, S., and Mucciardi, A.: Coarse root spatial distribution determined using a ground-penetrating radar technique in a subtropical evergreen broad-leaved forest, China, Science China. Life sciences, 56, 1038-1046, 10.1007/s11427-013-4560-7, 2013.

Zenone, T., Morelli, G., Teobaldelli, M., Fischanger, F., Matteucci, M., Sordini, M., Armani, A., Ferre, C., Chiti, T., and Seufert, G.: Preliminary use of ground-penetrating radar and electrical resistivity tomography to study tree roots in pine forests and poplar plantations, Funct. Plant Biol., 35, 1047-1058, 10.1071/fp08062, 2008.

Zhu, S., Huang, C., Su, Y., and Sato, M.: 3D Ground Penetrating Radar to Detect Tree Roots and Estimate Root Biomass in the Field, Remote Sens, 6, 5754-5773, 10.3390/rs6065754, 2014.

Table 1. A cross-study comparison of the detection capacity (minimum and maximum) of tree root diameter and depth in different soil types using GPR systems with various radar frequencies.

Radar frequency (MHz)	Tree species	Soil type	Site Condition	Detected root diameter (cm)		Detected root depth (cm)		Reference
				min	max	min	max	
400	*Pinus taeda*	Gergeville soil	Plantation	3.7	10	-	130	*Butnor et al., 2001.*
400	*Melaleuca quinquenervia*	Flat sandy soil	Controlled, root segments	3	13	-	50	*Nga et al., 2014*
450	*Quercus petraea*	Loamy deluvial soil	Plantation	3	5	-	200	*Hruska et al., 1999.*
500	*Larix kaempferi*	Forest soil	Plantation	-	10	10	30	*Zhu et al., 2014.*
500	***Quercus potosina, Pinus cembroides***	**Shallow, rocky soils**	**Semiarid tropical forest**	**2.5**	**7.5**	**3**	**40**	**This study**
500	*Ulmus pumila, Artemisia ordosica*	Dry sandy	Controlled, fixed sand dunes	-	3.5	10	80	*Cui et al., 2011.*
800	*Eucalyptus sp.*	River sand	Plantation	-	5	-	50	*Barton & Montagu, 2004(Barton and Montagu, 2004)(Barton and Montagu, 2004).*
800	***Quercus potosina, Pinus cembroides***	**Shallow, rocky soils**	**Semiarid tropical forest**	**0.6**	**4**	**1**	**40**	**This study**
900	*Prunus persica*	Faceville fine sandy loam	Controlled, peach orchard	2.5	8.2	11	114	*Cox et al., 2005.*
900	Different tree species	Red-yellow and marshy soils	Subtropical evergreen forest	1	3	1	60	*Yan et al., 2013.*
1,000	*Eucalyptus sp.*	River sand	Plantation	1	10	-	50	*Barton & Montagu, 2004*
1,000	*Quercus douglasii, Pinus sabiniana*	Auburn-exchequer soil	Semi-arid savanna	1.3	10	8	30	*Raz-Yaseef et al., 2013.*
1,500	*Populus deltoides*	Lakeland soil	Plantation	0.6	1.7	11	27	*Butnor et al., 2001.*
2,000	*Ulmus pumila, Artemisia ordosica*	Dry sandy	Controlled, fixed sand dunes	0.5	3.5	-	30	*Cui et al., 2011.*

Table 2. Number of trees per stand and species included in the study of soil water potential (*n*), as well as mean or tree diameter at breast height (DBH), age estimated based on rings growth and total tree height of trees of *Pinus cembroides* and *Quercus potosina* at Sierra San Miguelito, San Luis Potosí, Mexico.

Stand	***n***	**DBH (cm)**	**Age (years)**	**Tree height (m)**
Pine/pure	16	18.701 ±2.49	76.05 ±3.42	4.863 ±0.74
Oak/pure	16	21.104 ±1.67	83.17 ±3.21	5.272 ±0.86
Pine/mixed	16	19.981 ±1.76	84.20 ±4.88	6.080 ±1.17
Oak/mixed	16	20.121 ±1.38	82.06 ±2.82	5.461 ±1.08

Table 3. Calibration and validation of roots (diameter and depth). This table represents the information extracted from a radargram of a pine-oak stand, Fig. S4.

Along transect	***In situ***		**GPR 500 MHz**	
(m)	diameter (cm)	depth (cm)	diameter (cm)	depth (cm)
1.35	2.6	7.4	2.8	7.2
1.68	2.7	9.4	2.8	9.6
3.18	2.5	15	2.4	15.2
3.76	2.6	22.4	2.8	23.1
3.98	3.7	8.5	3.6	8.9
4.85	6.7	13.5	7.0	13.9
5.35	2.9	21.5	3.2	22.2
6.90	4.4	9.4	4.8	9.9
7.12	2.8	13.8	2.6	14.2
8.56	4.7	12.4	5.0	13.0
10.78	2.5	13.0	2.8	13.4
11.92	3.4	12.2	3.0	11.8

Table 4. Intercepts, slopes, regression coefficients and observed probabilities of linear regressions between root diameter (cm) and time interval (ns) which were used for calibration with both GPR systems for each sample type.

Type of sampling	**GPR systems**	**Stand**	**Intercept ± 1SE**	**Slope ± 1SE**	**R^2**	***P***
Radial	500 MHz	Pine	0.3610 ± 0.3751	5.7890 ±0.4473	0.92	<0.0001
Radial	500 MHz	Oak	-0.0013 ± 0.4234	5.7736 ± 0.4309	0.92	<0.0001
Radial	500 MHz	Mixed	-0.0536 ± 0.1506	6.0195 ± 0.1712	0.98	<0.0001
Concentric	800 MHz	Pine	-2.0910 ±0.1273	6.2450 ±0.1839	0.98	<0.0001

Table 5. Nested two-way analysis of variance to examine root diameter differences observed among the combination of four soil depths (10, 20, 30 and >30 cm) and three forest stands (*Pinus cembroides*, *Quercus potosina* and mixed forest) in a semiarid forest ecosystem in Central-North México.

Effect	**df**	***F***	***P***
Stand	2	8.51	0.0002
Depth (Stand)	8	184.98	<0.0001

5

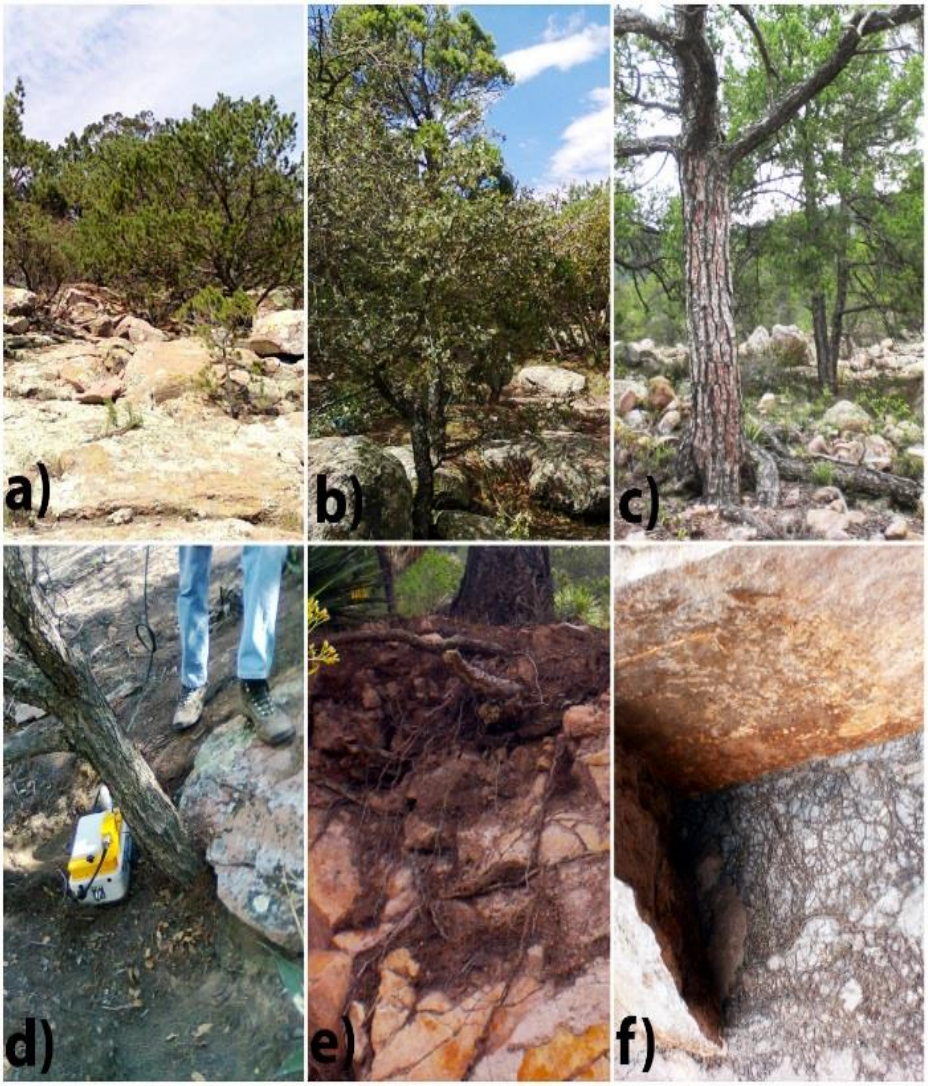

Figure 1. Site characteristics: (a) rhyolitic weathered bedrock in *Pinus cembroides* stands, (b) exfoliated rock in a pine-oak stand, (c) exposed coarse roots of 14 cm diameter in shallow rocky soils, (d) pine anchored under exfoliated rock, (e) high root density at the soil/bedrock interface, (f) fine roots colonizing a weathered bedrock layer.

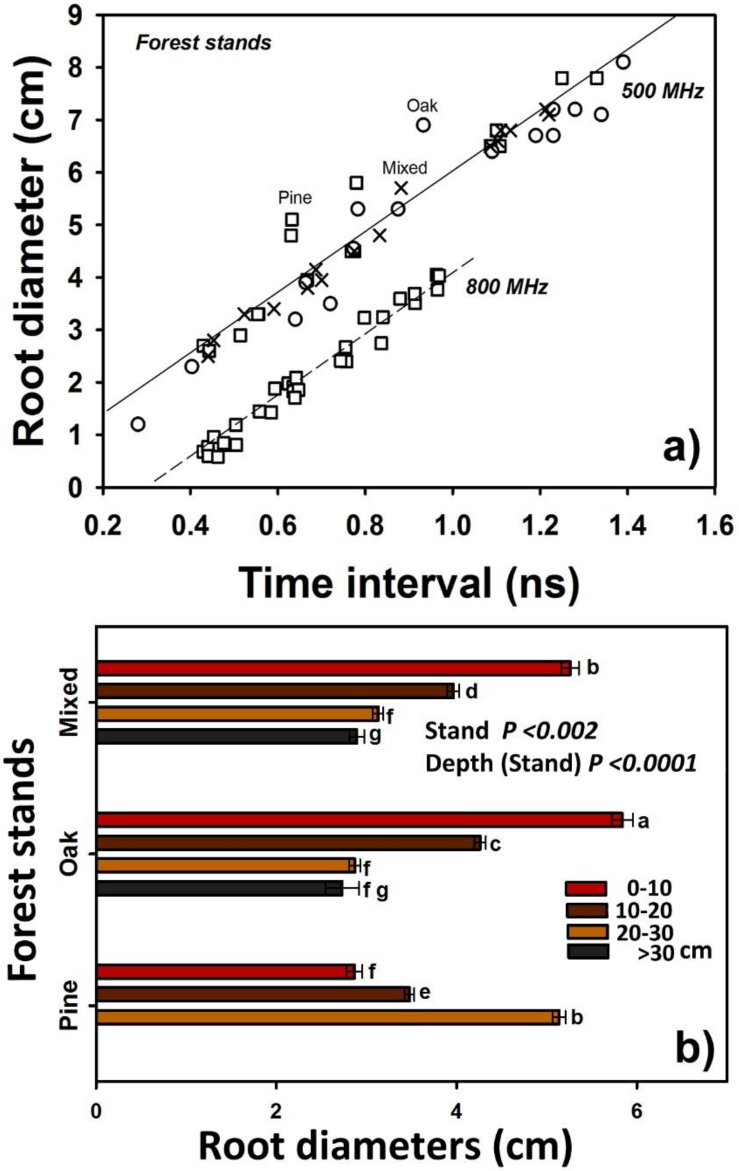

Figure 2. (a) Relationship between root diameter from different stands and time interval with zero crossing of detected roots, which were later used for calibration with both GPR systems: 500 MHz frequency antenna ($n = 48$), $P < 0.0001$, and 800 MHz frequency antenna ($n = 28$), $P < 0.0001$. (b) Average diameter of roots recorded with GPR for each of the three forest stand types at four depths. Different letters next to the bars indicate statistical differences among treatment combinations at a probability value of $P < 0.05$.

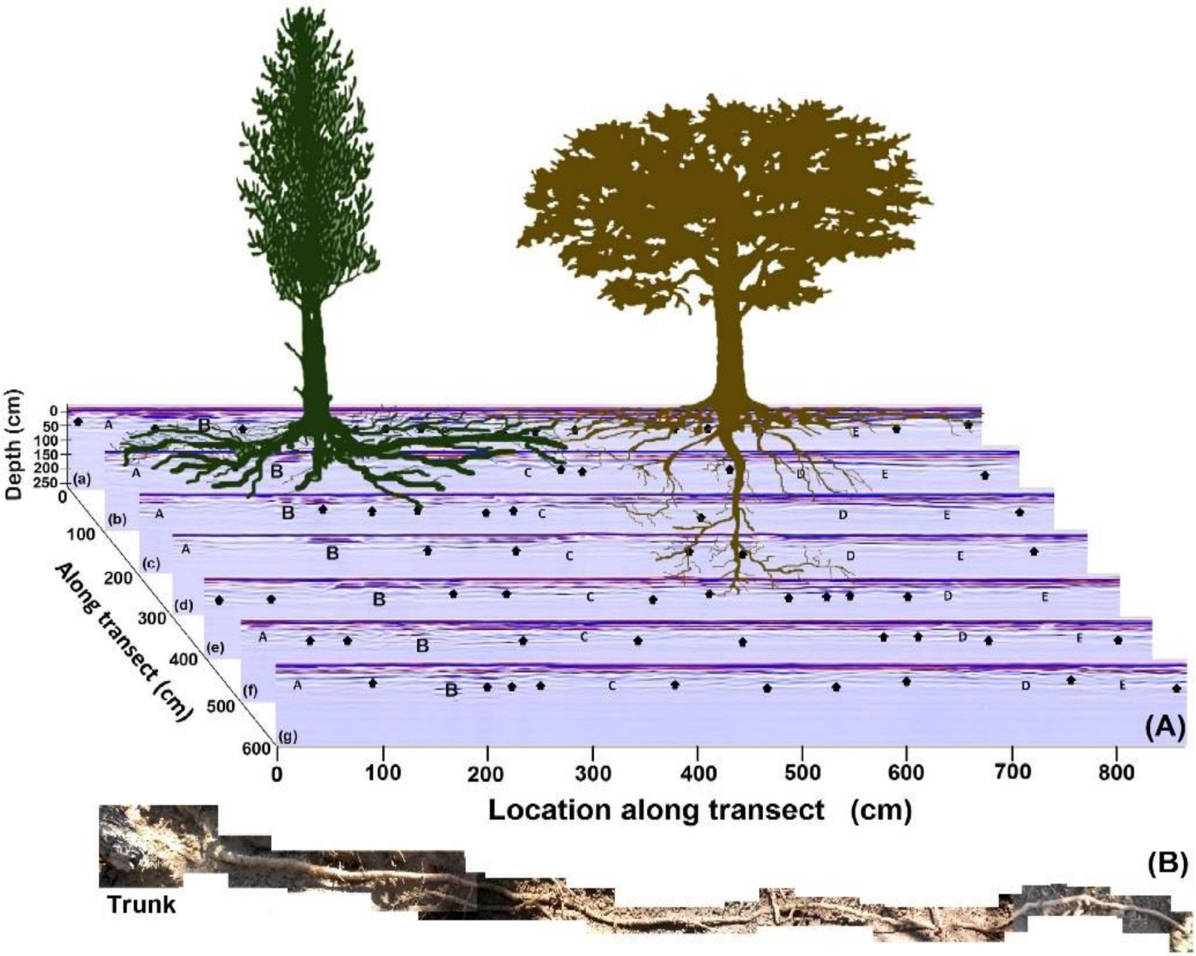

Figure 3. Mapping root systems with GPR show the potential for radargrams to represent an approximation of horizontal root distribution: (A) 2-D radargram sequence obtained with the 500 MHz antenna performing seven parallel transects of 8.5 meters, spaced 1 meter apart. In each radargram, cross-sections of roots were identified and then their diameters estimated. By linking root reflectors in neighboring GPR radargrams, the orientation and length of each single root were obtained (same letters). Arrows and letters in different GPR radargrams correspond to reflections from the same roots; they were used for calibration in situ. With the 500 MHz antenna the position, size, and depth of roots with 2.5 to 7.5 cm diameter were estimated. The image shows an example of the position of a pine and oak tree and the potential application of the GPR tool for spatially explicit root distribution studies. (B) Horizontal elongation of a root axis of *Pinus cembroides* marked with the letter "B" in (A).

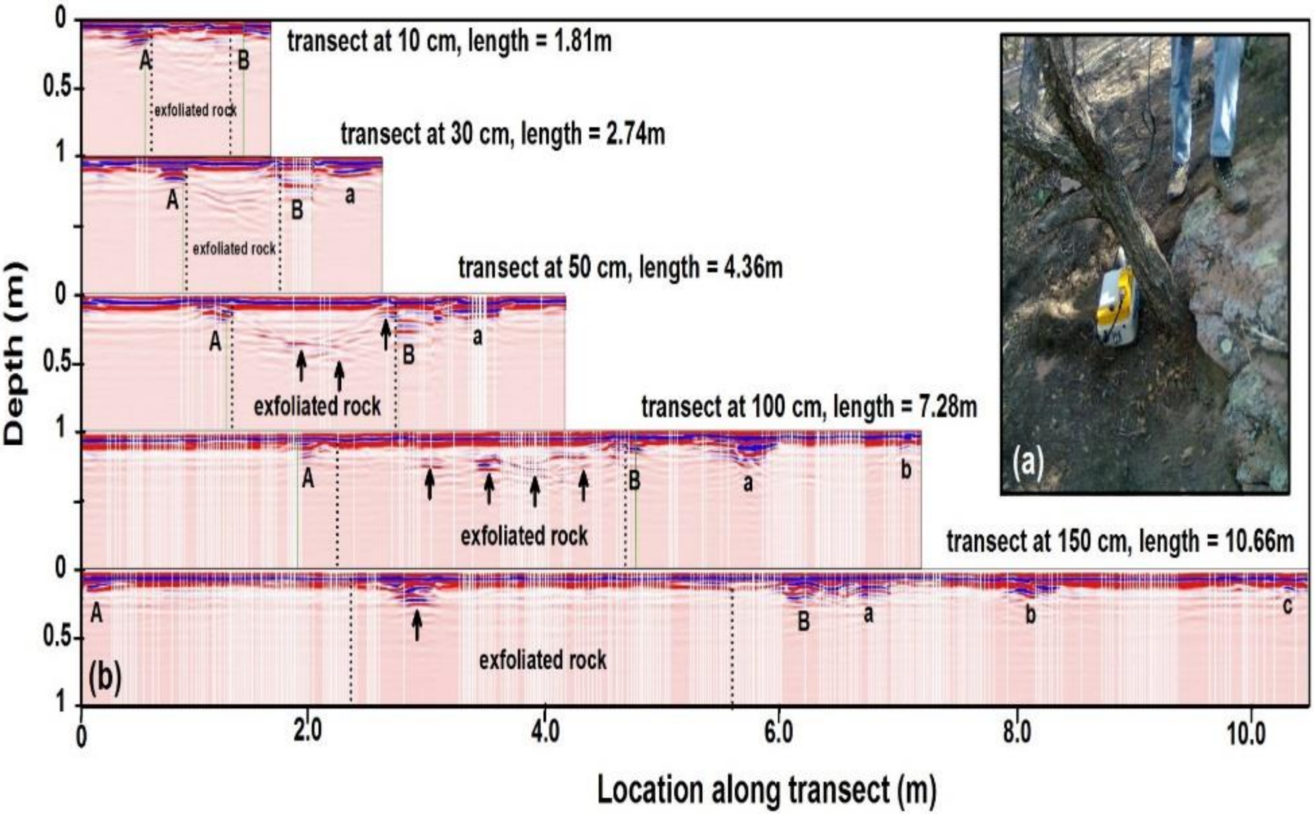

Figure 4. Concentric transects used to detect and track lateral root proliferation with GPR: (a) In situ photography showing a *Pinus cembroides* root anchored in exfoliated rock and the GPR system with the 800 MHz antenna. Five concentric transects were established around the tree with 0.1, 0.3, 0.5, 1.0 and 1.5 m distance between neighboring transects. The radius of each transect varied from 0.29 to 1.7 m; (b) Corresponding GPR radargrams of different transect lengths. Same letters in different GPR radargrams indicate examples of reflections from the same roots; uppercase letters indicate roots used for calibration. Arrows indicate root presence under exfoliated rocks.

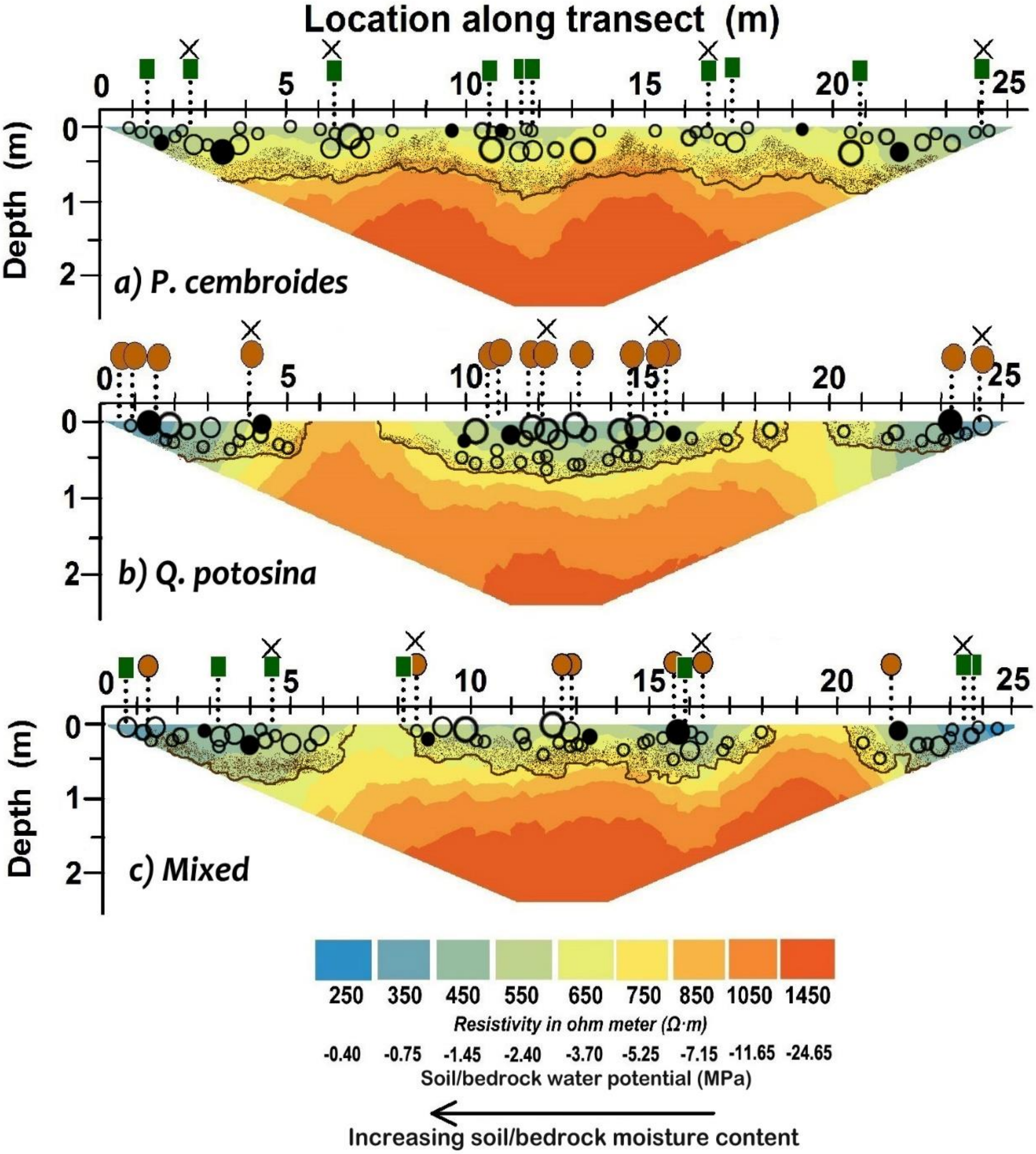

Figure 5. ETR tomograms in (a) *Pinus cembroides*, (b) *Quercus potosina* and (c) pine-oak forest stands. ERT profiles showed a relationship between the position of roots, low soil resistivity (greater water availability) and greater bedrock fracturing. The top soil corresponds to the first 20-25 cm layer, the intermediate layer includes soil pockets and rock fractures and is depicted by the dotted strip along the radargram and the fresh bedrock begins underneath the solid line. Circles of different size depict roots of different diameter size (see figure legend in Fig. S4). Black circles indicate roots that were used for GPR calibration. Trees marked with X indicate the presence of soil psychrometers sensors.

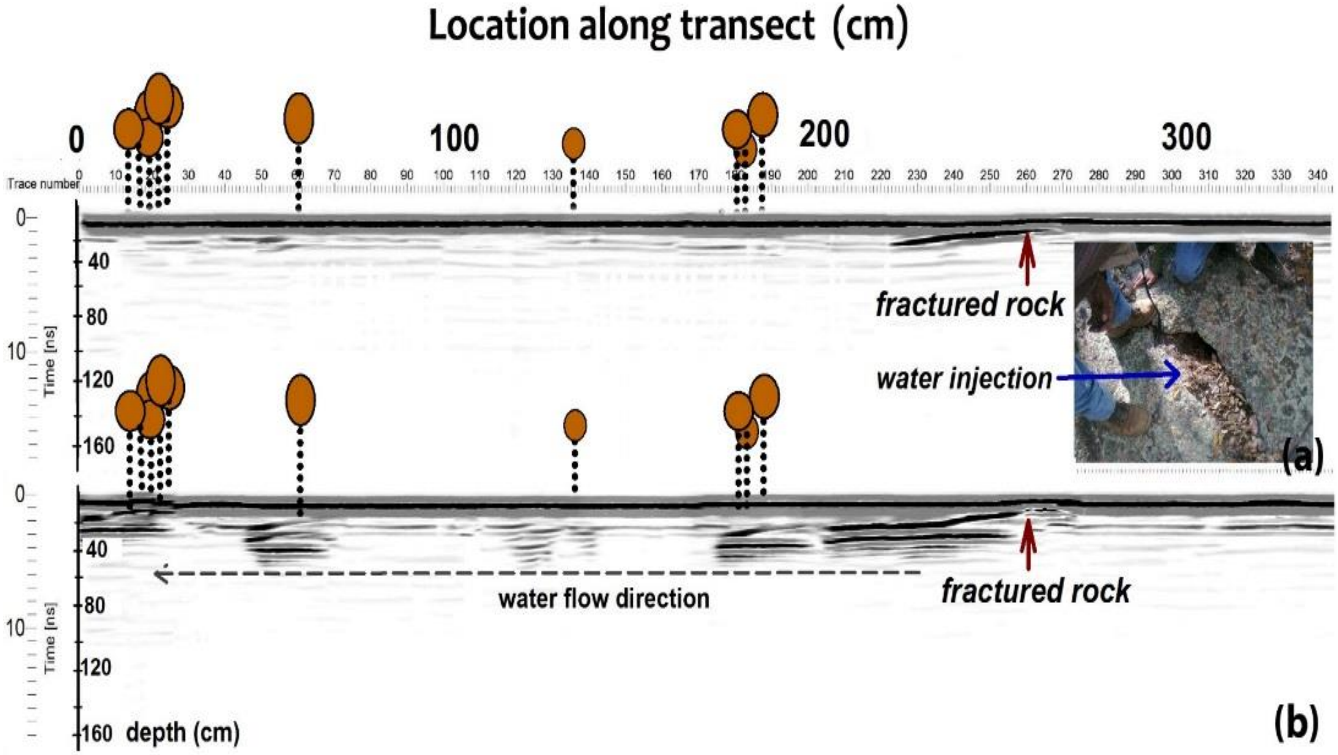

Figure 6. GPR radargrams showing how oak roots are preferentially located in fractured rocks where the probability of water accumulation is high. (a) GPR radargram in dry condition. (b) GPR radargram 150 minutes after the injection of 15 L of water in a rock fracture. In the radargrams filters were applied to highlight areas of interest. Inserted photo: rock fracture, where water was injected.